Harmful effects of strenuous exercise and possible medicinal interventions

0.Abstract

Strenuous exercise elevates the body's core temperature, which results in the appearance of heat stress conditions in the visceral organs, such as the intestine. Hence, there will be local ischemia and rapid reactive oxygen species production in the intestines, thus affecting the intestinal epithelial integrity and leading to several clinical symptoms. In this study, we exposed two groups (n=20) of male C57BL/6 N mice to different 6-week training regimes, a moderate and vigorous, and analyzed the morphological changes in the intestine. Strenuous exercise induced morphological changes in both exercised groups and it decreased ileal goblet cell population in the vigorous exercise group. Furthermore, there was a decrease in occludin expression and delocalization of this protein in both exercised groups in the colonic segments. We also observed a decrease in colonic ZO-1 expression in the moderate exercise group and an increase in colonic claudin-3 expression in the vigorous exercise group. As for the second part of the study, we exposed two groups (n=10) of male C57BL/6 N mice to the 6-week moderate exercise regime and introduced an antioxidant to the diet of each group, α-lipoic acid (ALA) and resveratrol. Interestingly, in the group feed with ALA, the strenuous exercise induced morphological changes found in the first study were not visible and ileal goblet cell population increased.

In conclusion, forced strenuous exercise leads to general inflammation, tight junction breakdown/delocalization and physical/functional changes of the several cells that compose the intestines. Antioxidants have shown to be an effective way to combat the damages caused by heat stress/hypoxia and it's pathways of action should be further studied in order to develop specific therapies that could help against this emerging problem.

1.Introduction

It is of general knowledge that regular exercise promotes physical and psychological wellbeing, however its detrimental effects are a topic that has remained vastly unexplored (1, 2). Recently there has been a rise on the research documenting the effects that exercise have on the intestine and the intestinal microbiota, which has been harnessing promising results and cause-effect associations that were unexpected (3). As an example, it has been documented that acute exercise might be harmful for gut integrity, which contrasts the several beneficial effects of chronic exercise (4).

Therefore, as the rise of recent literature suggests, gut integrity is of great importance, has it is vital for the wellbeing of the gut microbiota, which has been named as the new "organ" in the human body (5). This "organ" is a community of microbes that reside in the gut and have multiple interactions with different organs in the body (6), such as guaranteeing the homeostasis of the skin, impeding the initiation of pulmonary infections and developing and maturing the central nervous system (CNS)(7). This last interaction is called the gut-brain axis, its trough this

that the gut microbiota can inflict changes in the CNS, so if gut integrity is compromised, it can lead to deregulations in the composition of the gut microbiota which can affect the homeostasis of the brain and enhance the progression of CNS disorders and diseases(8.9).

The gastrointestinal tract is a complex and long system that encompasses a myriad of different organs (10). Two of them are the small and large intestine, which are divided in 4 distinct parts that appear in a descending order from the stomach, the duodenum, the jejunum, the ileum and lastly the colon (10). All these segments are composed by columnar epithelium cells, which have a function of nutrient absorption and secretion (11). This epithelium normally consists of closely packed single layer of cells that are more longitudinal than wide, giving it a stretched out columnar look (11). This epithelium (except in the colon) is composed by villi that extend onto to the luminal side and increase the mucosal surface area (12). Furthermore, the cells that compose this tissue derive from the crypts, which is where the intestinal stem cells reside and start their maturation and differentiation paths (12). The intestinal stem cells can differentiate into enterocytes (the cells responsible for the absorption of water and nutrients) and secretory cells such as enteroendocrine cells, Paneth cells and goblet cells (12). Goblet cells are a group of specialized epithelial cells that are capable of producing a mucus-like substance that could shield the cells from ROS (13). This mucus hydrogel is mainly composed of large mucin peptides, which have a barrier function, preventing microbial invasion of the lamina propria (14).

Several intestinal disorders have been linked with inducing morphological changes in the structure of the intestine, such as morphological abnormalities in chrohn's disease patients and general inflammation and presence of edemas in the lamina propria that occur in irritable bowel syndrome patients (15,16). Furthermore, recent literature has been showing us that diseases that weren't initially accredited as intestinal disorders can also cause lesions and morpho-histological changes in the intestine, namely how Parkinson's disease patients, a famous brain disorder, have a lower expression of occludin and different protein distribution occludin and ZO-1 (17). These proteins are tight junctions (TJs), which are special group of proteins that maintain gut integrity. These junctions promote a cell-to-cell adhesion between the epithelial cells that enables the segmentation of the luminal environment of the gastrointestinal tract and the basal lamina (18). Each protein possesses a unique function that interact together to form the network of proteins that are the tight junctions, for instance, claudins are a group of proteins that possess transmembrane and extracellular domains that are capable of forming networks of tight junction-like strands in the same cell and facilitate intercellular union(19).

The disruption of epithelium cells integrity can be induced through a myriad of ways, such as with the presence of pathogens, toxic substances and physical stressors, for example heat stress (HS), which has been gaining relevance and intensity in the past years due to the rise in global temperatures. HS affects the gastrointestinal track by switching the visceral blood flow to a peripheral circulation in order to dissipate the heat generated by skeletal muscle, in turn, this leads to a local ischemia and hypoxia condition, and following reperfusion, leading to the formation of reactive oxygen species (ROS) in visceral organs, such as the intestines (20). Due to their high reactivity, ROS are capable of inflicting changes in various different cellular macromolecules, such as lipids, nucleic acids and proteins (21).More specifically, ROS oxidizes the DNA, RNA and proteins and it causes lipid peroxidation in polyunsaturated fatty acids (22). These changes modify the cellular components of the cell, which will block these

macromolecules from exerting their normal functions (22). Therefore, high concentrations of ROS leads to damages in epithelium cells by disrupting the tight junctions that connect them, which creates a breach of the lamina proporia as the contents inside the luminal side, will go to the blood stream (23).

Strenuous exercise has been known to cause gut injury due to inducing intestinal ischemia, which increases intestinal permeability by damaging/dysfunctioning the tight-junction complex and also lead to a loss of function of all epithelial cells (24). From studying the concentration of intestinal fatty-acid binding protein (I-FABP), a biomarker for injury of mature enterocytes, it has been reported that vigorous endurance exercise at high temperatures leads to the highest concentration of this protein (24). This supports the idea that exercise at high temperatures is a strong promoter of exercise-induced gastrointestinal syndrome (EIGS), which leads to a myriad of intestinal complaints (25). EIGS has been known to induce clinical symptoms such as regurgitation, abdominal pain, diarrhea and fecal blood loss (24). Furthermore, despite having not yet been proven, strenuous exercise can theoretically exuberate intestinal problems in patients with chronic gastrointestinal problems, such as inflammatory bowel syndrome (IBS), as it would be adding more injuries to an already debilitated organ (24). In contrast, short low to moderate exercise has been proven to help patients that suffer from IBS (24).

The body has its own response mechanisms to stressful situations. Our previous study proved that colonic cells Caco-2/HT-29 that were exposed to 2 hours of hypoxia and high temperatures highly expressed 70 kilodalton heat shock protein (HSP-70), heat shock factor 1 (HSF-1) and nuclear factor erythroid 2 related factor 2 (Nrf2) proteins, which are key modulators of heat shock and oxidative stress resilience pathways (26). However, sometimes these defense mechanisms are not enough to stop ROS production and tissue damage will occur (27). Hence, it is important to find ways of bolstering ROS and persevering the body's natural redox balance. As such, the use of exogenous supplements, namely pre- and pro-biotics, polyunsaturated fatty acids, amino acids and antioxidants, are a promising way of maintaining gut integrity with each class of substances having its different benefits (20). The use of antioxidants as supplementation could be a solution to keep overproduction of ROS in check, as external pro-oxidants can enhance the Nfr2-Keap1 pathway redox ability (20). Due to their success in combating redox imbalances in other pathologies, α-lipoic acid (ALA), a fatty acid with antioxidant properties, and resveratrol (a plant polyphenol compound) were chosen as the substances to be used in this study (20).

In short, despite the rise of recent literature, there is no study that compares the intestinal morphological changes caused by two different intensities of strenuous exercises, with also elucidating on the beneficial effects of antioxidants in exercise-induced HS condition in the intestines. This paper achieved that by splitting the experiment into two batches. The first batch focused on studying the different effects of two groups with different intensities of strenuous exercise, a moderate exercise (5 running sessions/week) and a vigorous exercise (3 running sessions/week), on C57BL/6N mice intestines after a 6 week training regime. The second batch was used to explore the beneficial effects that two different antioxidants, Resveratrol and ALA, have on C57BL/6N mice intestines that have been exposed to the 6 week moderate exercise training regime. Several techniques such as Western Blot, immunofluorescence staining, Alcian

Blue staining and Hematoxylin & Eosin staining were performed to achieve the goals of this paper.

2. Materials and Methods

2.1. Animal and experimental design

Leiden University Medical Centre (Leiden, The Netherlands) provided us with 9-week-old male C57BL/6 N mice. Three distinct groups were formed after random division of the mice: control (CON, n = 20), moderate treadmill exercise (MOD-EX, n = 20), and vigorous treadmill exercise (VIG-EX, n = 20). The mice were housed in groups of 4 in cages that access to a filtered and ventilated air. They were maintained at temperature of 21 °C, humidity of 55%, with a 12 h light/dark cycle in a specific pathogen-free barrier facility, and had *ad libitum* access to a standard chow diet [RM3 (P), Special Diet Services, UK], along with pathogen-free water. The ingredients that compose the standard chow diet are listed as Supplementary Table S1. The food intake and body weight were assessed weekly before treadmill running session. All animal experimental protocol was approved by and performed under supervision of Leiden Animal Welfare Body (IvD Leiden), Leiden University (registration number PE.21.002.009, 31-05-2021).

In the second batch, six distinct groups of 9-week-old male C57BL/6 N mice were formed after random division: placebo (n=10), placebo with exercise (n=10), resveratrol (n=10), resveratrol with exercise (n=10), α-lipoic acid (n=10) and α-lipoic acid with exercise (n=10). The conditions of the mice were the same as in the first experiment. The exercised groups were subjected to the same training regime as MOD-EX from the first experiment. The ingredients that composed the placebo, resveratrol and α-lipoic acid diet are listed as Supplementary Info S1

2.2. Treadmill running exercise protocol

The mice were allowed 10 days of acclimation to the environment prior to the beginning of the exercise training. After the acclimation period, the mice were familiarized to the 5-lane rat treadmill (Maze Engineers) by undergoing a 3-day progressive exercise training regime that was adapted to the MOD-EX and VIG-EX mice, when the speed and incline of the track were incrementally increased each day. No more than 4 cage mates were allowed to run on one lane of the treadmill together. In order to guarantee induced exercise throughout the whole experiment, the mice were kindly pushed back on to the belt with a brush when they dropped off the track. The fixed training regime started from day 4 of training, where the MOD-EX group ran 5 times a week with a 15 min warm-up followed by 45 min at 16 m/min all at 5º slope. While the VIG-EX group ran 3 times a week at 5º slope with a 5 min warm-up before enduring 25 min at 23 m/min. In order to ensure the animals were always induced with strenuous exercise, the speed of the training regime was raised twice throughout the whole experiment. Firstly, starting from day 15, the speed of both exercise groups was elevated by 1m/min. Secondly, starting from day 29, the speed of the VIG-EX group was risen by 1m/min. The comprehensive treadmill running program is found as Supplementary Table S2 and S3.

2.3. Rectal temperature

The mouse rectal thermometer (BAT-12, Physitemp Instruments, USA) was used weekly to access the rectal temperature. In order to have an accurate reading, the mice underwent a 15-min break from the treadmill exercise session, before the probe was gently inserted into 1 cm of the mouse rectum. Prior to each insertion, the probe was sterilized with 75% ethanol.

2.4. Tissue collection and pretreatment

After the mice autopsy, 2 cm of the jejunal, duodenal, colonic and ileal segments were harvested and cleaned with cold sterile PBS. The spleen was isolated and weighed. All tissue samples were immediately frozen in dry ice and kept at -80ºC until further use.

The 5-cm Swiss rolls were made following Carol *et al.*'s method (28), with the proximal small intestine starting from c.a. 4 cm to the pylorus, the distal small intestine (till c.a. 2 cm to the cecum) and colon (starting from c.a. 2 cm to the cecum). Aftewards the Swiss rolls were fixed in cold 3.7% formaldehyde solution (104003, Sigma-Aldrich, USA) for a minimum of 48 hours and then transferred to 70% ethanol, prior being embedded in paraffin.

2.6 Preparation of slides with samples for Histology

Samples from the duodenal, jejunal, ileal and colonic segments of mice intestines underwent trough the 16 hour program from the tissue embedding machine Leica TP 1020 and subsequently were impregnated in paraffin blocks using the Leica EG 1150C. The Paraffin blocks were stored in a cold room (4ºC) until later use. Finally, the blocks were cut into 5 µm thick sections using the microtome Leica R M2165 and were sampled into slides.

2.7 Deparaffination of Slides with samples impregnated in paraffin

Firstly, the slides were immersed in the first xylene compartment for 5 minutes followed by immersion in the second xylene compartment for 5 minutes. Afterwards the slides underwent immersion in ethanol solutions in a decreasing order of concentration for 3 minutes each, starting with ethanol 100% two times, then ethanol 96%, followed by ethanol 90%, ethanol 70% and lastly ethanol 50 %. Finally, the slides were immersed in demi water for 3 minutes, they can be kept in it up to 2 hours.

2.8 Alcian Blue and Nuclear Fast Red Staining

In order to access the percentage of goblet cell population in the mice's intestinal vilis duodenal, ileal and colonic segments were stained with Alcian Blue. After the deparaffination step, the slides were incubated in 3% acetic acid for 3 minutes and followed by staining with Alcian Blue solution for 35 minutes, which is responsible for the staining of the nucleus and goblet cells. Consequently, the slides were washed in running water until the effluent was clear and counterstained in nuclear fast red solution for 4 minutes. In order to remove the excess fluid, the slides were immersed 20 times in distilled water, 50% EtOH and 70% EtOH. Afterwards, the slides were rinsed for 2 min in 90% EtOH, 96%EtOH and two times in 100% EtOH. Finally the slides were rinsed two times in xylene for 2 min and mounted with mounting solution (1:1 of xylene and pertex), in order to preserve the staining the slides were covered with a glass plate.

2.9 Hematoxylin & Eosin Staining

Primarily, the slides underwent the deparaffination step. Consequently, they were immersed in hematoxylin for 5 minutes and rinsed for 5 min in running tap water until the effluent is clear and the Hematoxylin stained parts turn from the original aubergine(eggplant) color into blue, which stains the nuclei a purplish blue color. Subsequently, the slides were stained with Eosin Y working solution for 2 min and 30 seconds, giving the extracellular matrix and cytoplasm pink color. Excess fluid removal and mounting of slides was the same process as in the Alcian Blue staining.

2.10 Histomorphological evaluation

After the Hematoxylin & Eosin staining, the inflammation, epithelial change and mucosal architecture of the samples were evaluated and scored by double-blinded technicians, according to the modification of Erben *et al.*'s guide (29). For this, just one picture from each slide was shot and scored representing one individual mouse. The scoring scheme is presented as Supplementary Table S4 and S5. The length of each villi was measured using Fiji of ImageJ software (NIH, USA). Three random villi were measured from each field and the mean of these villi lengths represented the inputted value for each field. The slides that were stained with Alcian Blue and Nuclear Fast Red had the goblet cells and epithelium cells in each villus located and counted.

2.11 Immunofluorescence staining

Immunofluorescence staining was performed in order to localize the tight/adherent junction proteins. Firstly, in order to remove the paraffin, the 5-µm sections were rinsed two times for five minutes each in Xylene and Ethanol 100%. Consequently, they were incubated for 30 min with 0.3% H_2O_2 solution in methanol to block endogenous peroxidase activity. After gradient rehydration and rinse with PBS, the slides were incubated in boiling sodium citrate buffer (pH 6.0) for 10 min, then cooled down with an ice bath for 1 hour in the sodium citrate buffer. The slides were rinsed with PBS again and blocked with 5% goat serum in PBS containing 1% bovine serum albumin (BSA) for 30 min at room temperature, then incubated overnight with primary antibodies of occludin (1:100, #404700, Invitrogen, USA), claudin-3 (1:100, #341700, Invitrogen, USA) and E-cadherin (1:100, #BD610182, BD Biosciences, USA) at 4 °C. After the incubation of the primary antibodies, the slides were rinsed and incubated with Alexa-Fluor fluorescently conjugated secondary antibodies (1:1000, Invitrogen, USA) for 1 h at room temperature. Lastly, the slides were mounted and the nuclei were counterstained with ProLong Gold Antifade Mountant with DAPI (#P36935, Invitrogen, USA). The cover-slipped cells were visualized by confocal microscopy system (TCS SP8, Leica, Germany). Rabbit IgG polyclonal isotype control (#ab176094, abcam, UK) were used for occludin and claudin-3 antibodies, and mouse IgG isotype control (#550878, BD Biosciences, USA) was used for E-cadherin antibody.

2.12. In-vivo Sample Preparation for Western Blot

Tissue colonic segments were rinsed with PBS in cold. Afterwards, they underwent lyses and homogenization by Precellys 24 homogenizer (Bertin Instruments, France) using Precellys

lysing beads at 6000 rpm, 10 s × 3 cycles, with cold Pierce RIPA buffer (Thermo Fisher Scientific, USA) containing protease inhibitor cocktail (#11836170001, Roche, Switzerland). Lastly, the samples were centrifuged at 12000 rpm for 10 minutes and the resulting supernatant was collected. The Pierce BCA Protein Assay Kit (Thermo Fisher Scientific, USA) was used in order to assess and standardize the total protein concentration.

2.13. Western blotting (WB)

Equal amounts (50 μg) of boiled protein samples were loaded onto the gel (Criterion Gel, 4-20% Tris-HCL, Bio-Rad, USA) in a casting tray submersed with 1x running buffer. Ladders were added to both sides, with the right side having double the amount in order to establish a direction in the gel. Subsequently, the mix of proteins were separated by electrophoresis using Bio-Rad's PowerPac HC at around 130 Volts for 60-90 minutes and electro transferred onto Trans-Blot Turbo polyvinylidene difluoride (PVDF) membranes (midi format 0.2μm, Bio-Rad, USA) using Bio-Rad's Trans-Blot Turbo system. The membranes were rinsed several times with PBS-T before being blocked with 5% skimmed milk in PBS containing 0.05% Tween-20 (PBST) for one hour. Afterwards, the membranes went through another round of rising and were incubated overnight at 4 ℃ with the primary antibodies of occludin (1:500, #404700, Invitrogen, USA), claudin-3 (1:1000, #341700, Invitrogen, USA), E-cadherin (1:500, #14-324982, Invitrogen, USA) and ZO-1 (1:500, #339100, Invitrogen, USA). In the next day, the membranes were again rinsed multiple times with PBS-T and then incubated with correspondent horseradish peroxidase (HRP) -conjugated secondary antibodies (1:10000, Dako, Denmark) for 2 hours at room temperature. After being rinsed well with PBST and incubated with ECL detection reagent (#RPN2235, GE Healthcare, USA), the membranes were exposed to ECL imaging system (ChemiDoc MP, Bio-Rad, USA). The optical intensity of the blots was recorded and analyzed by using Image Lab (version 6.01, Bio-Rad, USA) and ImageJ (version 1.80, NIH, USA) software. Housekeeping proteins β-actin (1:2000, #13E5, Cell Signaling, USA) were assessed in parallel with each target protein and used for normalization.

2.14. Statistical analysis

Unless stated otherwise, all results are indicated as means ± SEM and have a sample size of ten (n=10). GraphPad Prism software (version 9.3.1, GraphPad, USA) was used to perform all statistical analyses. Unless otherwise stated, the differences between each group were determined using ne-way analysis of variance (ANOVA) with Bonferroni post-hoc test. These differences were considered statically significant when $p<0.05$.

3. Results

3.1. 6 weeks of strenuous exercise decreases Goblet Cell population in intestinal villi

Alcian Blue staining was conducted to examine the effects of exercise on the villous goblet cell population in mouse duodenal and ileal segments. Illustrative images let us see the goblet cell population and size on the ileal segments (Fig.1A). It is visible that the VIG-EX group has smaller and less goblet cells in the villi than the CON group (Fig.1A). In consequence, in the ileum segments, vigorous exercise significantly decreased the percentage of Goblet cells in

the villi (Fig.1B). However, in the duodenal segments, we can observe that exercise did not significantly affect the population of goblet cells (Fig1.B).

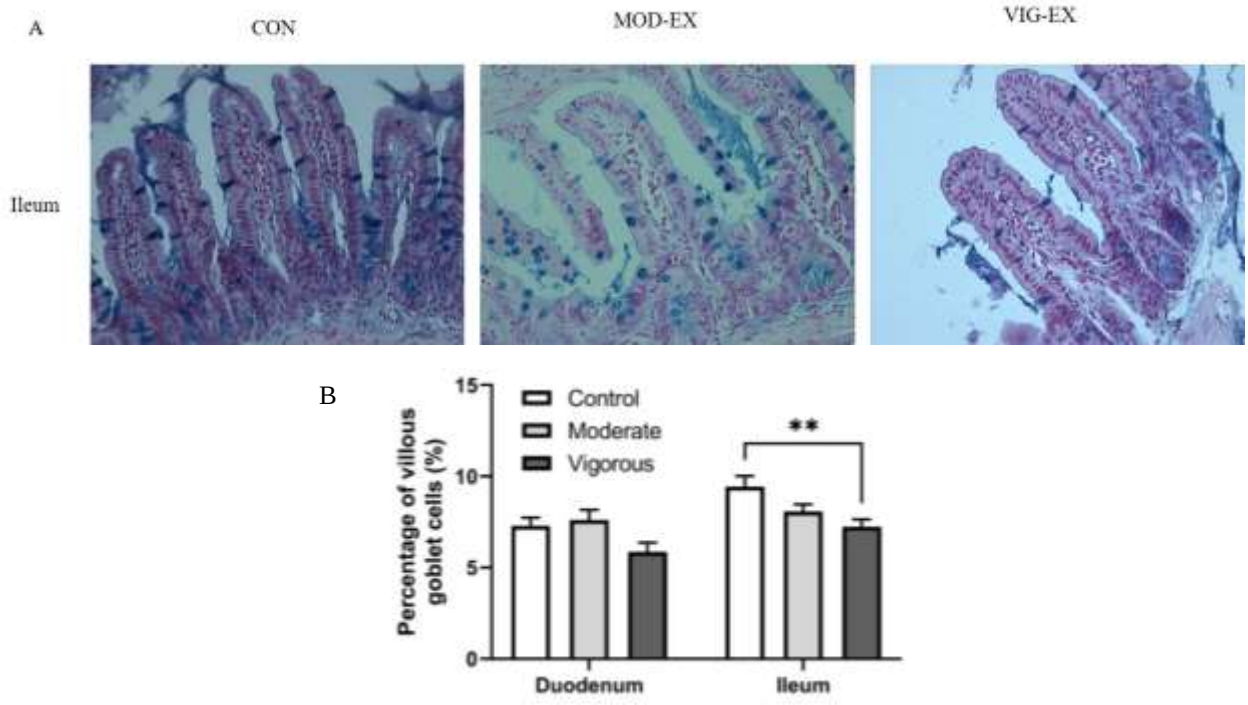

Figure 1.A) Representative images of ileal segments stained with Alcian Blue and Nuclear fasta red elucidate the increase goblet cell population and size in each group. The following images were captured using the Olympus BX50 microscope with UPlanFI 40× /0.75 objective lens and Leica DFC320 10× camera **B)** Percentage of villous goblet cells from the duodenal and ileal segments. Statistical differences were analyzed by one-way ANOVA followed by the Bonferroni's multiple comparison test.** $p<0.01$. CON: Control; MOD-EX: Moderate Exercise; VIG-EX: Vigorous Exercise.

3.2 6 weeks of a diet rich in α-lipoic acid, with and without moderate exercise, increases Goblet Cell population in intestinal villi

Alcian blue staining was conducted to assess the effects of a diet rich in antioxidants, with and without exercise, on the population of villous goblet cells. Illustrative images show us the goblet cell population and size in the ileal segments (Fig.2-A). It's possible to see that there are more goblet cells throughout the whole mucosa in the ALA groups and that these cells seem more packed with mucin granules (Fig.2-A). In the ileal segments, we can observe that a diet rich in ALA significantly increases the percentage of villous goblet cells with and without moderate exercise (Fig.2-B). In contrast, a diet rich in resveratrol did not produce any significant differences in comparisons to the control (Placebo) group (Fig.2-C). As for the duodenal segments, neither resveratrol nor ALA feed groups produced significant differences to placebo groups (Fig.2-D, 2-E).

A

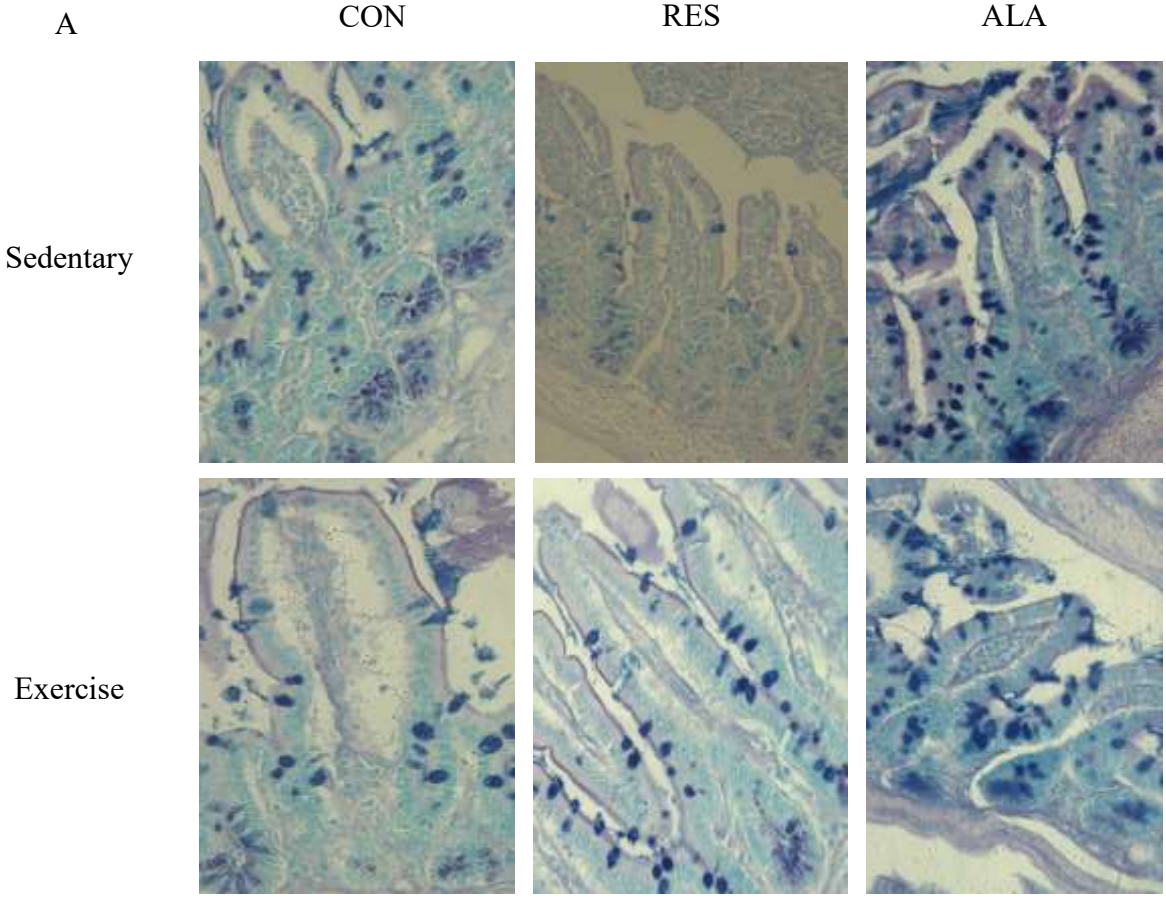
CON
RES
ALA
Sedentary
Exercise

B

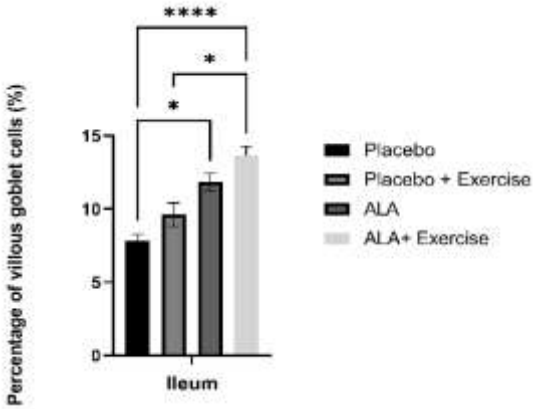
****
*
*
Percentage of villous goblet cells (%)
15
10
5
0
Ileum
Placebo
Placebo + Exercise
ALA
ALA+ Exercise

C

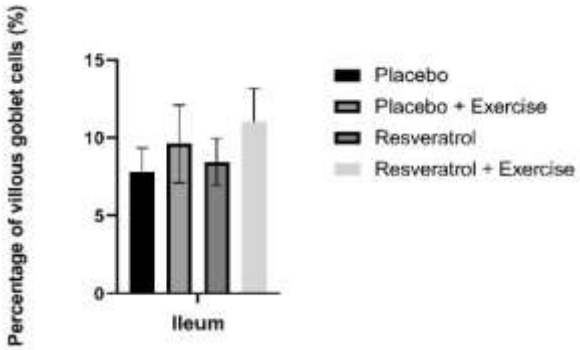
Percentage of villous goblet cells (%)
15
10
5
0
Ileum
Placebo
Placebo + Exercise
Resveratrol
Resveratrol + Exercise

D

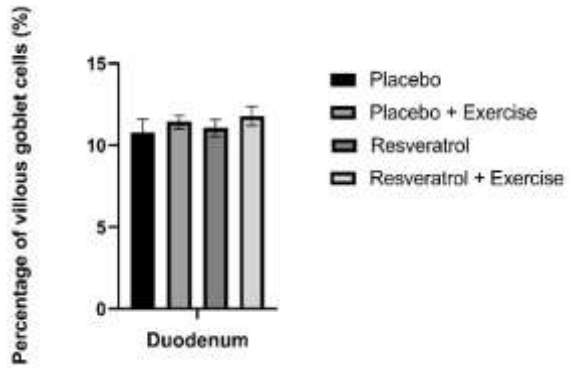
Percentage of villous goblet cells (%)
15
10
5
0
Duodenum
Placebo
Placebo + Exercise
Resveratrol
Resveratrol + Exercise

E

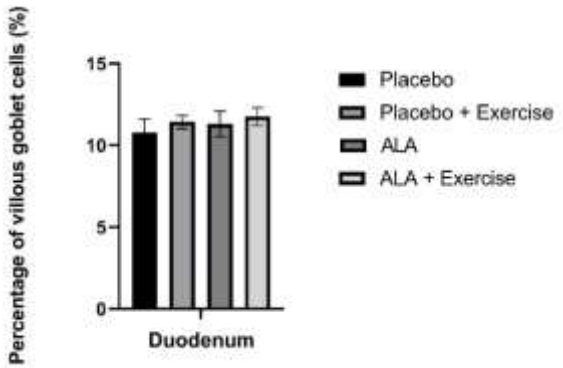
Percentage of villous goblet cells (%)
15
10
5
0
Duodenum
Placebo
Placebo + Exercise
ALA
ALA + Exercise

Figure 2. **A)** Representative images of ileal segments stained with Alcian Blue and Nuclear fasta red elucidate the increase goblet cell population and size in each group. The following images were captured using the Olympus BX50 microscope with UPlanFI 40× /0.75 objective lens and Leica DFC320 10× camera **B)** Percentage of villous goblet cells from the ileal segments of the control and ALA feed groups. **C)** Percentage of villous goblet cells from the ileal segments of the control and resveratrol feed groups. **D)** Percentage of villous goblet cells from the duodenal segments of the control and resveratrol feed groups **E)** Percentage of villous goblet cells from the duodenal segments of the control and ALA feed groups. Statistical differences were analyzed by one-way ANOVA followed by the Bonferroni's multiple comparison test.* $p<0.05$, **** $p<0.0001$. ALA: α-lipoic acid; RES: Resveratrol; CON: Placebo.

3.3. 6 weeks of strenuous exercise changes intestinal morphology and induces local inflammation in mice.

We examined mouse duodenal, ileal and colonic sections to determine the effect of strenuous exercise on intestinal morphology. We used H&E staining, which is standard to examine inflammatory responses in animal models, to determine the effects of strenuous exercise on intestinal histomorphology in mouse duodenal, ileal and colonic sections. By using Erben *et al.*'s guide (29) we were able to meticulously evaluate intestinal morphological change which was divided into 3 main categories: Inflammatory cell infiltrate, epithelial change and mucosal architecture. The scoring system used is attached as Supplementary Table S4 and S5. In the control group most villi are in normal shape, extending from base to tip without any critical change (Fig. 3-A). The presence of inflammatory infiltrates was minimal and submucosal and mucosal architure remained undisturbed, as such, the morphological score in all CON segments was low.

In all segments, both moderate and vigorous exercise groups produced some kind of morphological change, such as mucosal or submucosal infiltration of leukocytes, submucosal edema, hemorrhage, ulceration, blunted villus and submucosal widening (Fig. 3-A). These morphological changes were high enough to produce significant differences between control and moderate exercise in all 3 sites (Fig.3-C). As for the vigorous exercise groups, there were only significant morphological changes in the duodenal and ileal segments (Fig.3-C). Lastly, moderate exercise significantly decreased duodenum villus length (Fig.3-B), which can be observed in Fig.3-D.

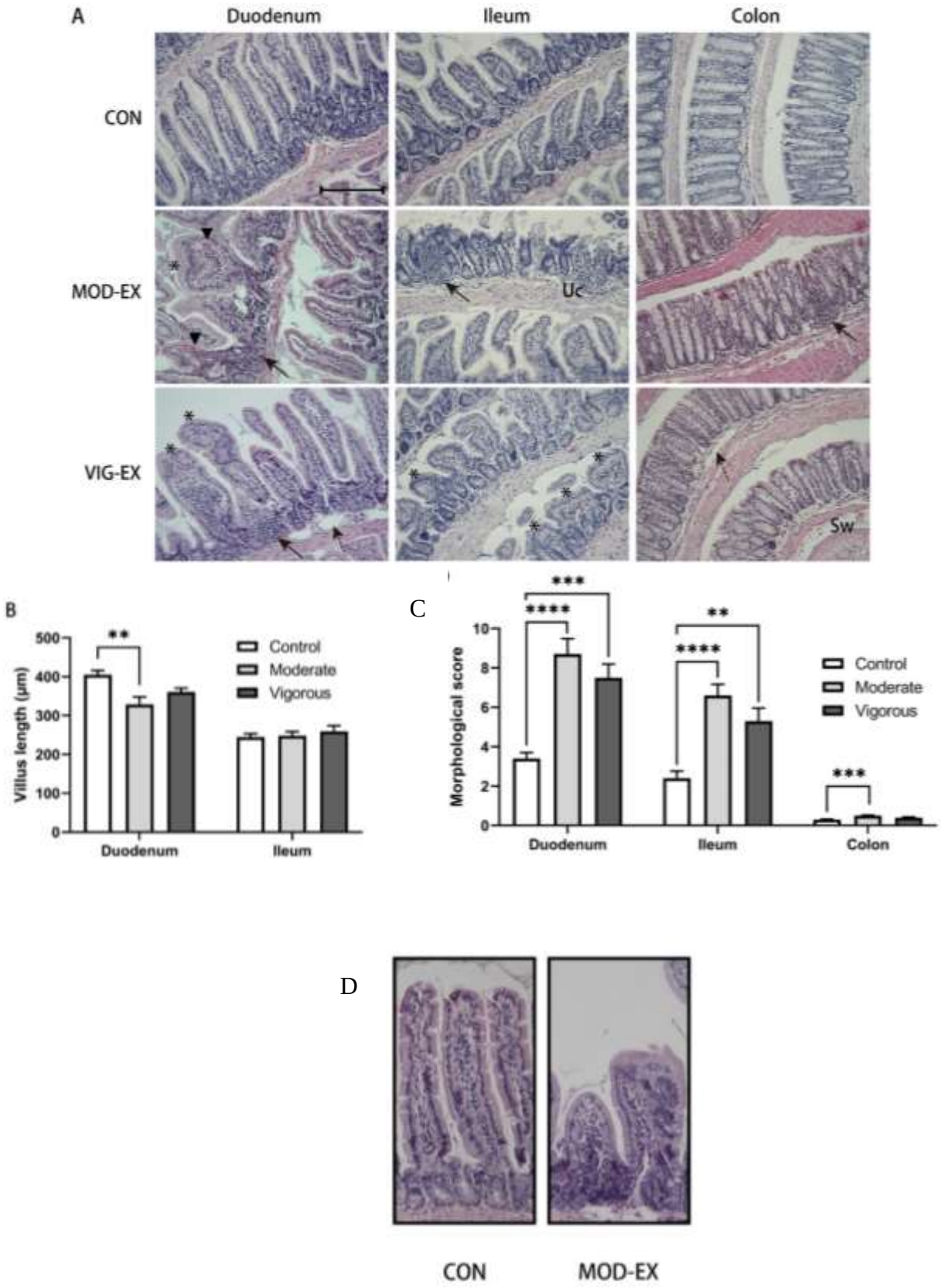
A
Duodenum
Ileum
Colon
CON
MOD-EX
VIG-EX
Uc
Sw
B
Villus length (μm)
Control
Moderate
Vigorous
Duodenum
Ileum
C
Morphological score
Control
Moderate
Vigorous
Duodenum
Ileum
Colon
D
CON
MOD-EX

Figure 3. (**A**)Illustrative images of ileal, colonic and duodenal sections stained with H&E elucidate the mucosal and sub-mucosal infiltration of the inflammatory cells, the modifications in the epithelia and the changes in the mucosal architecture. The following images were captured using the Olympus BX50 microscope with UPlanFI 20× /0.5 objective lens and Leica DFC320 10× camera (200×, scale bar 200 μm). Solid arrow: mucosal or submucosal infiltration of leukocytes; dashed arrow: submucosal edema; arrow head: hemorrhage; Uc: ulceration; asterisk: blunted villus; Sw: submucosal widening. (**B**) Villus lengths (**C**) Histological scores for intestinal morphological change. (**D)** Representative images of duodenal villi, showing the different villus lengths. Data are presented as the mean ± SEM; n = 10 per group. Statistical differences were analyzed using one-way ANOVA followed by the Bonferroni's multiple comparison test. ** $p<0.01$, *** $p<0.001$, **** $p<0.0001$. CON: Control; MOD-EX: Moderate Exercise; VIG-EX: Vigorous Exercise.

3.4 6 weeks of strenuous exercise influences relative intensity and pattern of tight junction proteins.

Immunofluorescent staining was conducted for the tight junctions OCLN, CLDN3 and adherens junction E-cad to further clarify their localization in the epithelia. However, the sections stained with CLDN3 and E-cad antibodies only showed a difference in intensity between the control and exercise groups, with the tight junction distribution remaining unchanged (Supplementary Figure S2). In contrast, the colonic segments that were stained with OCLN presented structural differences between control and exercise groups. In Control, the OCLN proteins formed a ring pattern in the cross-sectional villi and a net like pattern in the longitudinal villi (Fig.4-A) Furthermore, compact columnar cells were organized in a brush-like structure on the corona of the villus. Both strenuous exercised groups clearly disrupted cellular distribution of OCLN and decreased the number of column cells in mouse colonic villi (Fig. 4-A). When observing the cross-sectional villi it is also possible to notice a disconnected and asymmetrical pattern of OCLN with visible clusters of concentrated cytosolic proteins. We also applied this staining with the occludin antibodies to the duodenal and ileal sections, however, the illustrative results are not as impressive as colon (Supplementary Figure S3). We also performed an isotype and secondary antibody control of the immunofluorescence staining, which are illustrated in Supplementary Figure S2. We also conducted WB, to determine the relative intensity of OCLN, CLDN3 and ZO-1. Both moderate and vigorous exercised diminished OCLN protein expression in mouse colonic segments, confirming the damage of the epithelial integrity (Fig.4-B). In addition, we also found that moderate exercise decreased colonic ZO-1 protein expression, while vigorous exercise increased CLDN3 protein expression (Fig. 4-B, 4-C).

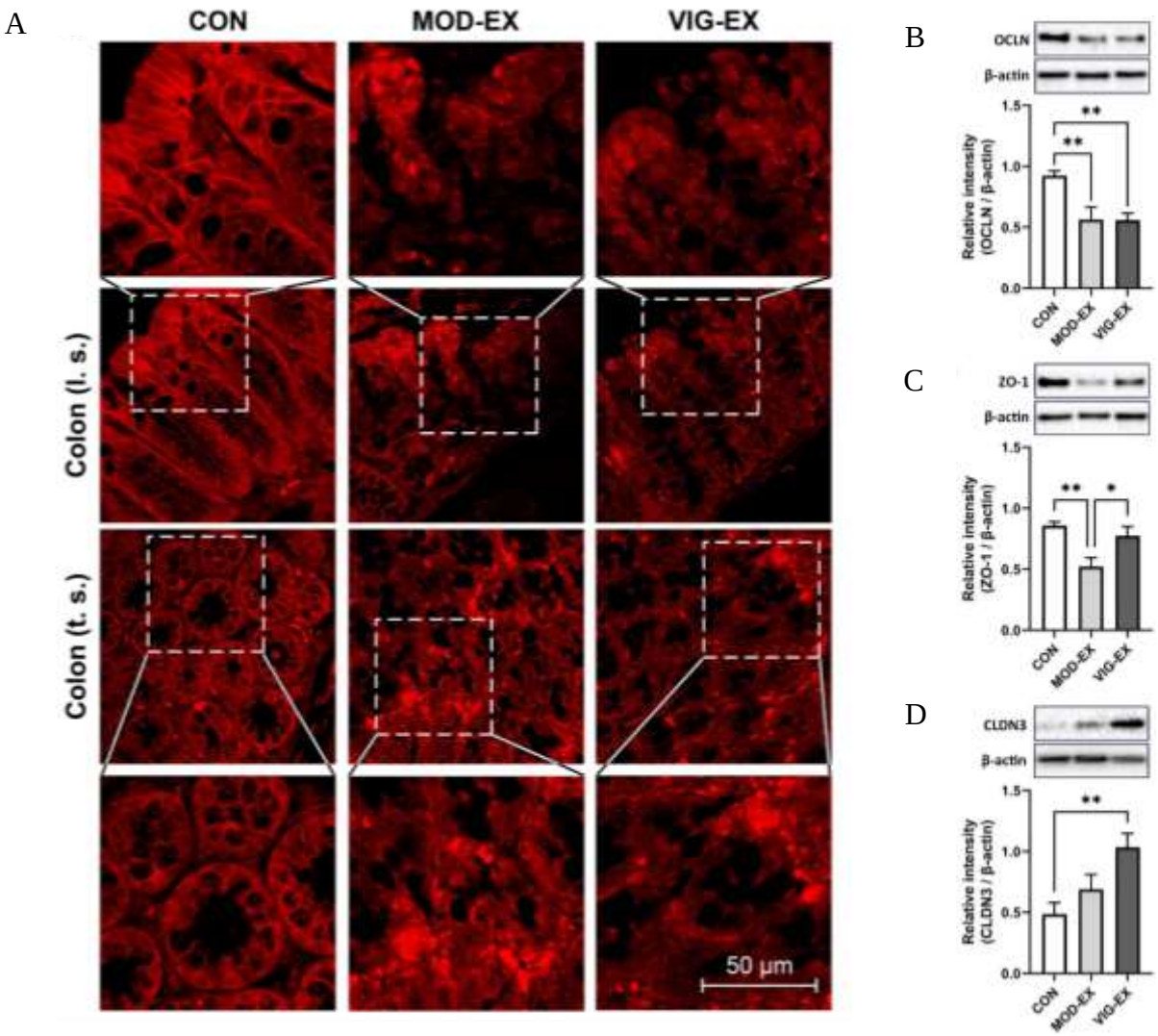

Figure 4. (**A**) Immunofluorescence staining of colonic occludin protein with a cross-sectional and longitudinal viewpoint. The Leica TCS SP8 confocal microscope with HCX IRAPO L 25×/0.95 objective lens at 2.25× digital magnification was used to obtain these pictures; pinhole: 1.50 AU. The red colour in the images are the fluorescent signals from Alexa-Fluor 594 secondary antibodies. (**B, C, D**) Western Blot data showing the relative protein expression of colonic claudin-3, occludin and ZO-1 normalized with β-actin expression.. Data are presented as mean ± SEM; n = 10 per group. Statistical differences were analyzed by one-way ANOVA followed by the Bonferroni's multiple comparison test. * $p<0.05$, ** $p<0.01$. CON: Control; MOD-EX: Moderate Exercise; VIG-EX: Vigorous Exercise; l.s.: longitudinal section; t.s.: transverse section; CLDN3: claudin-3; OCLN: occludin; ZO-1: zonula occludens-1.

3.5. Strenuous exercise elevates rectal temperature

Throughout the 6 weeks of treadmill training regime, the rectal temperature of control group hovered around the baseline with no significant change (Fig. 3-A). In contrast ,the rectal temperatures of moderate and vigorous exercise groups were significantly increased after exercise compared to the sedentary mice and reached a maximum of around 39 °C, which was around 1 °C higher than CON (Fig. 5). However, the rectal temperature was similar between the two exercise groups.

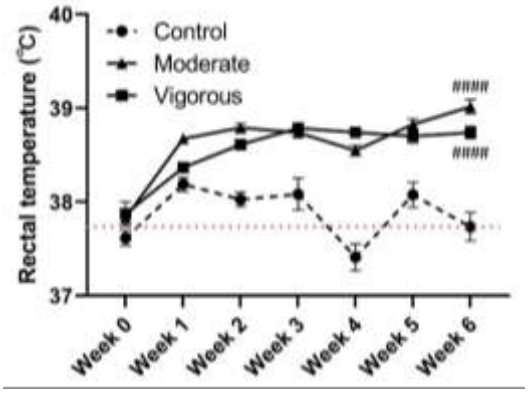

Figure 5. (**A)**Rectal temperature of the mice after exercise. The baseline is represented as the red dotted, which was set as the average rectal temperatures of all groups of mice at week 0 (37.77 °C). Data are presented as mean ± SEM; n = 20 per group. Statistical differences were analyzed by one-way ANOVA followed by the Bonferroni's multiple comparison test. #### $p < 0.0001$ vs Control.

3.6 ALA reduces the morphological change caused by 6 weeks of strenuous exercise

We examined mouse duodenal, ileal and colonic sections to determine the effects of ALA and Resveratrol, with and without strenuous exercise on intestinal morphology. In both placebo and resveratrol group it was possible to see that the strenuous exercise produced some kind of visible morphological change trough blunted villus, submucosal widening, submucosal edema, infiltration of leukocytes and ulceration in all segments (Fig.6-A). However, these changes were not as visible/common in the exercised ALA fed mice in any segment (Fig.6-A). As such, the exercised ALA fed mice, were the only exercised group that had significantly lower morphological score than the placebo exercised mice in all segments (Fig.6-B).

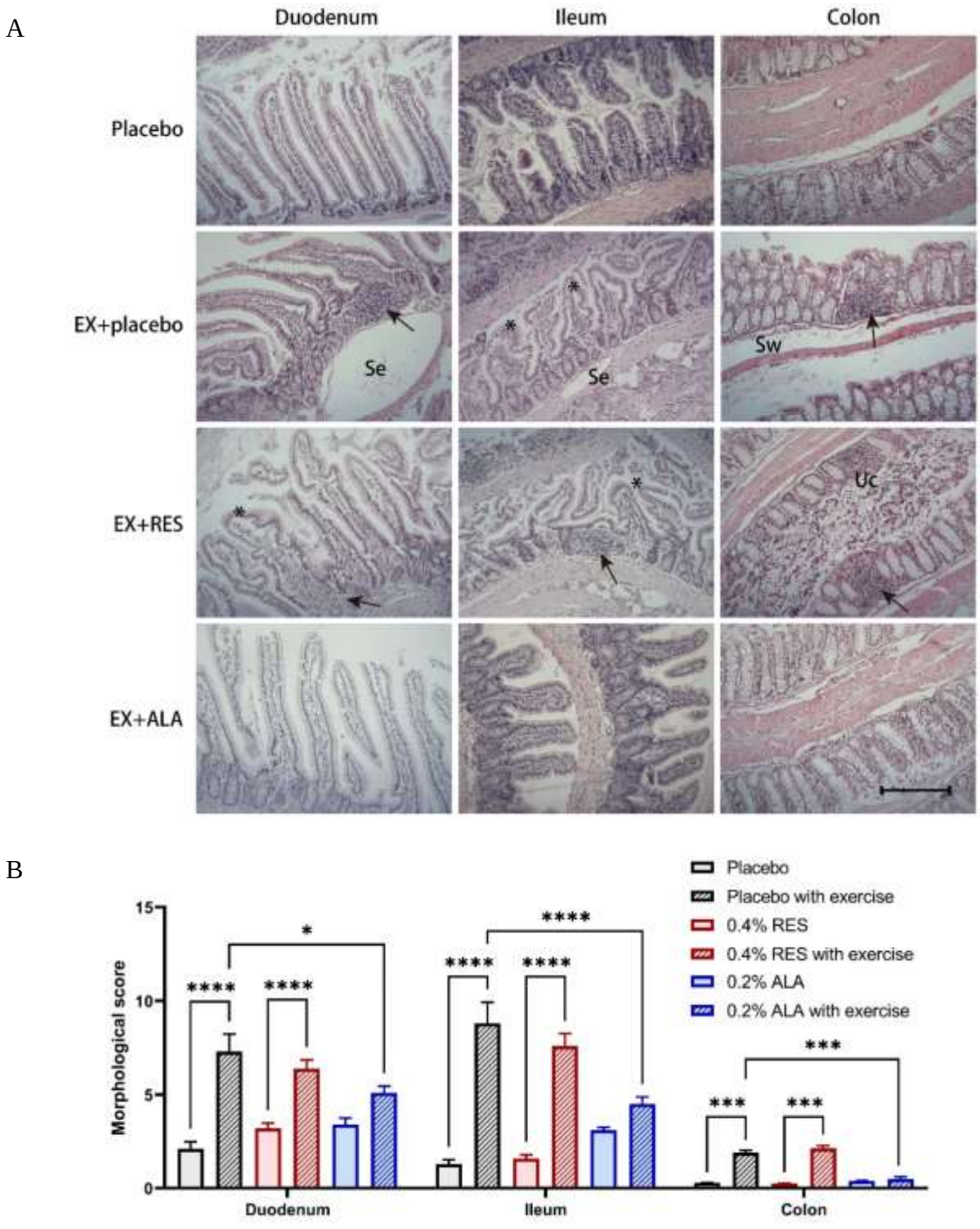

Figure 36 (**A**) Illustrative images of ileal, colonic and duodenal sections stained with H&E elucidate the mucosal and sub-mucosal infiltration of the inflammatory cells, the modifications in the epithelia and the changes in the mucosal architecture. The following images were captured using the Olympus BX50 microscope with UPlanFI 20× /0.5 objective lens and Leica DFC320 10× camera (200×, scale bar 200 μm). Solid arrow: mucosal or

submucosal infiltration of leukocytes; SE: submucosal edema; Uc: ulceration; asterisk: blunted villus; Sw: submucosal widening. (**B**) Histological scores for intestinal morphological change. Data are presented as the mean ± SEM; n = 10 per group. Statistical differences were analyzed using one-way ANOVA followed by the Bonferroni's multiple comparison test. * $p<0.05$, *** $p<0.001$, **** $p<0.0001$. RES: Resveratrol; ALA: α-lipoic acid.

4. Discussion

Firstly, it is important to note that the mice underwent forced treadmill exercise. Forced treadmill exercise is known to induce stress responses that can counteract the beneficial anti-inflammatory effects of exercise on mice (30). Furthermore, a study on the effects of voluntary wheel running and low to moderate forced treadmill running in C57Bl/6J mice, which were subjected to DSS-induced colitis, showed us that the forced exercise (FE) aggravated inflammation and colitis symptoms, while voluntary exercise (VE) did the exact opposite (31). In Cook, et al (31) they found that thymus and adrenal weights significantly decreased and increased, respectively, in the FE group and the there was no change in weight between the VE group and control group, this confirmed that the mice in the FE were under more stress. Additionally, the VE mice ran further distances than the FE, so it all points out to the forced aspect of the exercise, which stressed the mice (31). Stress is known to induce peripheral and central inflammation and to have a synergistic effect in inflammatory bowel disease patients, so when conducting forced exercise experiments, indices of chronic stress should be measured, such as but not only, thymus and adrenal gland weight(32,33). Hence, since there was evidences of resistance to run from some mice, it is possible that part of the intestinal inflammation observed in the exercise groups was due to stress and not the exercise itself. Additionally, the vigorous exercise (Vig) group were more resistant to running than the moderate (Mod) group, as these mice were pushed to their limit of exercise, so it would be expected that this group was more stressed than the Mod group. However, this cannot be accounted when making significant claims as chronic stress wasn't measured in this study.

It is known that stress can induce structural changes in intestines, with chronic stress decreasing the population of goblet cells in the intestines (34). Alcian blue staining is a technique that allows to stain material that is inside mucin-bearing structures (35). As such, this staining can stain goblet cells, as they are columnar epithelial cells that can produce and secrete a variety of different mucins, such as MUC2 (36). All these mucins form the mucus that goblet cells secrete, which acts has a barrier between the luminal contents and epithelial cells, protecting the intestinal cells from the bacteria or other harmful pathogens (14).This is detrimental to keep epithelial cells integrity. This staining yielded some promising results, as goblet cell population significantly decreased in ileal segments on mice that were subject to the vigorous exercise regime. This goes in hand with the findings of Gomes *et al* (37), where exercise decreased Goblet cell population in rat's jejunal segments. Due to an increase in crypt depth and villous thickness in their study, Gomes *et al* (37) extrapolated that exercise increased cell proliferation into the crypts and differentiation into types of enterocytes that are not goblet cells. Another possible explanation could be that the expected higher ROS production in the vigorous exercise group led to a higher mucin secretion that could reduce the concentration of mucins in goblet

cells, making them not visible through alcian blue staining (38). Furthermore, exercise did not affect goblet cell population in the duodenum segments, this could be due to the fact that the population of goblet cells increases throughout the gastrointestinal tract and that the GSH antioxidant system plays a less important role in the distal parts of the small intestine (39, 40). This data hints to goblet cells having a protective role against free radical species that is more prevalent in the distal segments of the intestine. Brownlee *et al* (41), already has documented this protective role against free radicals like ROS. With the data from the second batch, it is possible to see that ALA increases goblet cell population and seems to form bigger and mucin packed goblet cells. ALA is a very strong antioxidant that is capable of scavenging ROS and act as pro oxidant (42). Furthermore, mucin accumulation in the goblet cells is directly dependent on ROS production by autophagosomes and the NADPH oxidase complex (13). Hence, combining the data from this study and what we know from literature, it is possible to infer that ALA could increase mucin accumulation due mimicking the beneficial effects of ROS and also increase goblet cell proliferation and differentiation in the ileum. However, there is still lack of literature and understanding about the effects of exogenous substances in the mucin accumulation pathway, so this pathway should be studied in mice with a diet rich in ALA to really conclude if it improves mucin accumulation.

The Hematoxylin and eosin (H&E) staining is a well refined process that allows us to get a myriad of structural information from tissues that are embedded in paraffin, as such, it is perfect to a access the effects of exercise in the intestinal structure (43). In addition, it is necessary to have a scoring system in order to correctly assess these structural changes, so through double-blinded technicians we were able to quantify the inflammatory response and changes in the epithelium and mucosal architecture, according to the modification of Erben *et al.*'s guide (29). Our results showed that moderate exercise produced morphological changes to colonic, ileal and duodenal segments, while vigorous exercise only produced significant changes in duodenal and ileal segments. Furthermore, the moderate exercise group in duodenal segments produced a significant decrease in villus length when compared to control and moderate exercise groups exhibited a trend of higher morphological change when compared to vigorous exercise groups in all segments. We know exercise can have a myriad of effects, these are dependent on the duration and intensity of exercise, with mild to moderate exercise normally having beneficial effects (protecting against colon cancer, diverticular disease, cholelithiasis, etc), contrasting acute strenuous exercise, which may provoke gastrointestinal bleeding, nausea, abdominal pain, etc (44). Adaption to the strenuous exercise regimes can be achieved and this mitigates the harmful effects in the intestine (45). However, in our study, strenuous exercised was always induced on the animals, so the possibility that the mice fully adapted to the training regime, making it an easy task, is not taken in consideration. Hence, it is possible to infer that a regime of longer and more frequent moderate exercise inflicts more damage in the intestine than a shorter and less frequent vigorous exercise regime. This claim is backed by the fact that rectal temperature, expression of heat stress transcription factor HSF-1 and gut permeability were similar in both moderate and vigorous exercise groups and significantly different to control (Supplementary Figure S5). Furthermore, the concentration of serum CRP, which measures tissue damage, was only significantly different to control in the moderate exercise group **(**Supplementary Table S5). This data leads us to hypothesize that the moderate exercise group

was exposed to a similar level of heat stress as vigorous exercise group, thus it was the increased time and frequency of exposure to conditions of hypoxia that increased the intestinal structural changes. The same experiment should be repeated and intestinal ROS levels in all segments should be measured in order to confirm this hypothesis. Lastly, the moderate exercise group ran always 230 meters more per day than the vigorous exercise group, however there is no literature on the correlation of distance covered and intestinal damage. Therefore, a study with multiple groups running at the same intensity but with slight variances of time would elucidate the effects of distance covered and time of exercise on intestinal damage.

From the second batch of H&E staining, our morphological score results showed that, in all segments, the mice that were feed with ALA and exercised had a significantly lower morphological score than the placebo group that exercised. Hence, strenuous exercise didn't structurally change the intestinal mucosa in the mice that had a diet with ALA. Furthermore, the intestinal leakage of the exercised ALA feed group wasn't significantly different from the sedentary group, as it had a trend of being lower when compared to sedentary groups, this only cements ALA's beneficial properties in intestines against heat and oxidative stress (Supplementary Figure S7). Additionally, CRP serum concentration, which is a clinical marker for inflammation, remained unchanged for both ALA and resveratrol feed mice between the sedentary and exercised groups (Supplementary Figure S6) (46). This data confirms the antioxidant capability of both substances, leading us to hypothesize that both substances are able to interact with ROS produced during exercise and reduce these species, which leads to a decrease in reactive species and intestinal inflammation (47).

Indirect immunofluorescence (IF) staining is a technique that allows for the visualization of many cellular components through the use of primary antibodies that connect to the desired target and secondary antibodies attached to a fluorophore that will exhibit fluorescence (48). Despite staining duodenal, ileal and colonic segments with CLDN3, ZO-1 and OCLN antibodies, only the colonic samples stained with OCLN produced significant changes in protein distribution relative to the exercise groups. Occludin is a tight junction protein that posses' many functions and pathways that regulate tight junction that are not totally understood and proven yet (49). However, there has been some recent developments in literature that are trying to explain the functionality of this protein, such as it's influence in regulating the paracellular flow of large molecules(50). Occludin is also responsible on forming the tight-junction branching points and controlling the complexity of the tight junction network, this last role determines which molecules can pass through the tight junctions (51). Manda (49), showed in her dissertation that occludin is a protein that posses' a regulatory motif (ORM) which confers dynamic properties to tight junctions trough phosphorylation dependent protein-protein interactions. She also hypothesized that oxidative stress in the epithelium leads to the activation of the tyrosine kinase c-Src, which will phosphorylate tyrosine in the ORM region, enabling its connection to a microtubule through the epithelial specific microtubule MAP7 and it's cofactor Kinesin-1. Furthermore, the phosphorylation of occludin is also responsible for the opening and closing of tight junctions, therefore any miss phosphorylation of occludin will directly affect membrane permeability (52).Lastly, it is thought that tyrosine phosphorylated occludin could dissemble from the tight junctions and be degraded in the proteasome, this is evident in patients that suffer from inflammatory bowel syndrome (53). This leads me to hypothesize that the exercise groups

in the colonic segments were in the presence of oxidative stress due to the high ROS production during strenuous exercise, which lead to the internalization of the phosphorylated occludin in caveolin-1, this can be observed in the cytosolic clusters of occludin present in the exercise groups (54). Additionally, the decrease in occludin protein concentration in both exercise groups found trough Western Blot also suggests there was occludin degradation, so it supports Coeffier et al's (53) claim of an increase of proteasome-mediated degradation of occluding during the inflammatory response. Also, has mentioned above, the GSH antioxidant system plays a less important role throughout the gastrointestinal tract, therefore the distal parts of the intestine will be subjected to more ROS during exercise, which supports our findings of higher occludin degradation and internalization in colonic segments in comparison with ileum and duodenum segments (40).

Claudins are a family of 24 different mammalian claudins that are the main component of tight junction (TJ) strands, which create an ion-selective barrier between the apical and basolateral compartments (55). Claudin-3 is a tight junction protein from this family that we choose to observe due to its role on tightening the TJ strands, with overexpression of claudin-3 leading to an increased paracellular resistance of cations in cation-selective MDCK II cells (55). Nonetheless, claudin-3 is highly interactive with other claudins and its' barrier function is dependent on the concentration of other claudins, such as claudin-1,-2 and -5 (55). In our study, claudin-3 expression was significantly increased in the vigorous exercise group, which contrasts the evidences of downregulation of claudin-3 expression during inflammatory response (56, 57). However, claudin-3 overexpression has been observed in colorectal adenocarcinoma cell lines and tissues, indicating that it could be a potential histopathological biomarker for colorectal cancer (58). In addition, it has been reported that the development colorectal cancer is upregulated by the generation of ROS during the later stages of the inflammatory response (59). Hence, it is a possible that the overexpression of claudin-3 in the vigorous exercise group was caused due to the presence of colorectal adenocarcinoma cells in the mice's colon.

The zonula occludens (ZO) are group of three proteins that are responsible for TJ formation and function by connecting other TJ proteins, such as occludin and claudin, to the actin cytoskeleton (60). We choose to examine ZO-1 as it seems to be the most important zonula occluden, as cells that lack ZO-1 have delayed activity of occludin and claudin, despite maintaining an intact structure of the tight junctions and showing no evidences of increased permeability (60). When we analyzed this protein through western blot it illustrated that the moderate group yielded a significant decreased when compared to both control and vigorous exercise groups. This was a curious result, as it would be expected that the vigorous exercise would also decrease ZO-1. However, we know that the loss of ZO-1 proteins occurs before the presence of inflammation in DSS induced colitis in female BALB/c mice, so the loss of this tight junction is a boosting factor in increasing gut permeability (61). Therefore, as moderate exercise group was the only group with significant morphological damages in the colon, it would be expected that ZO-1 expression would be lower in this group.

Despite running Western Blot with samples from all intestinal segments, only the colonic segments yielded results. Even though there is no literature about ZO-1' expression throughout the Gastrointestinal tract, it is known that claudin-3 expression is higher in rats colon when compared to other segments and mRNA expression of occludin achieves its' maximum in

C57BL/6J's mice colon (62, 63). Hence, it could be possible that the colon has a higher concentration of these tight junction proteins when compared with other intestinal segments.

In conclusion, forced strenuous exercise elevates the body's core temperature, which leads to local ischemia in the visceral organs due to the heat stress condition. Consequently, there might be an increase in ROS production in the intestines, which leads to general inflammation, tight junction breakdown and delocalization and physical/functional changes of the several cells that compose the mucosa and sub-mucosa. The use of supplements containing antioxidants as shown to be an effective way to combat the damages caused by heat stress and it's pathways of action should be further studied in order to develop specific therapies that could help against this emerging problem. Furthermore, in the future, microbiota composition should be checked in order to see how these structural changes effect the gut the microbiota.

5.References

1. Adamu, B., Sani, M. U., & Abdu, A. (2006). Physical exercise and health: a review. *Nigerian Journal of Medicine*, *15*(3), 190-196
2. Edwards, S. (2006). Physical exercise and psychological well-being. *South African journal of psychology*, *36*(2), 357-373.
3. Donati Zeppa, S., Agostini, D., Gervasi, M., Annibalini, G., Amatori, S., Ferrini, F., … Stocchi, V. (2019). *Mutual Interactions among Exercise, Sport Supplements and Microbiota. Nutrients, 12(1), 17.* doi:10.3390/nu12010017
4. Keirns, B. H., Koemel, N. A., Sciarrillo, C. M., Anderson, K. L., & Emerson, S. R. (2020). Exercise and intestinal permeability: another form of exercise-induced hormesis?. *American Journal of Physiology-Gastrointestinal and Liver Physiology*, *319*(4), G512-G518.
5. Sinha, Anirban. (2020). Gut Microbiome: The New Organ?. Hormone and Metabolic Research. 5. 01-02
6. Blaser, M. J., Cardon, Z. G., Cho, M. K., Dangl, J. L., Donohue, T. J., Green, J. L., ... & Brodie, E. L. (2016). Toward a predictive understanding of Earth's microbiomes to address 21st century challenges. *MBio*, *7*(3), e00714-16.
7. Anwar, Haseeb & Irfan, Shahzad & HUSSAIN, Ghulam & Faisal, Muhammad & Muzaffar, Humaira & Mustafa, Imtiaz & Mukhtar, Imran & Malik, Saima & Ullah, Muhammad. (2019). Gut Microbiome: A New Organ System in Body. 10.5772/intechopen.89634.
8. Sharon, G., Sampson, T. R., Geschwind, D. H., & Mazmanian, S. K. (2016). The central nervous system and the gut microbiome. *Cell*, *167*(4), 915-932.
9. Cussotto, S., Sandhu, K. V., Dinan, T. G., & Cryan, J. F. (2018). The neuroendocrinology of the microbiota-gut-brain axis: a behavioural perspective. *Frontiers in neuroendocrinology*, *51*, 80-101.
10. Penninck, D., & d'Anjou, M. A. (2008). *Gastrointestinal tract* (pp. 281-318). Ames, Iowa: Blackwell publishing.-A
11. Ovalle, W. K., & Nahirney, P. C. (2020). *Netter's Essential Histology: With Correlated Histopathology*. Elsevier Health Sciences.
12. Allaire, J. M., Crowley, S. M., Law, H. T., Chang, S. Y., Ko, H. J., & Vallance, B. A. (2018). The intestinal epithelium: central coordinator of mucosal immunity. *Trends in immunology*, *39*(9), 677-696.
13. Campbell EL, Colgan SP. Control and dysregulation of redox signalling in the gastrointestinal tract. *Nat Rev Gastroenterol Hepatol*. 2019;16(2):106-120. doi:10.1038/s41575-018-0079-5
14. Birchenough, G. M., Johansson, M. E., Gustafsson, J. K., Bergström, J. H., & Hansson, G. (2015). New developments in goblet cell mucus secretion and function. *Mucosal immunology*, *8*(4), 712-719.

15. D'Incà, R., Sturniolo, G. C., Martines, D., Di Leo, V., Cecchetto, A., Venturi, C., & Naccarato, R. (1995). *Functional and morphological changes in small bowel of crohn's disease patients. Digestive Diseases and Sciences, 40(6), 1388–1393.* doi:10.1007/bf02065556 -1
16. D'Incà, R., Sturniolo, G. C., Martines, D., Di Leo, V., Cecchetto, A., Venturi, C., & Naccarato, R. (1995). *Functional and morphological changes in small bowel of crohn's disease patients. Digestive Diseases and Sciences, 40(6), 1388–1393.* doi:10.1007/bf02065556 -2
17. Clairembault, T., Leclair-Visonneau, L., Coron, E., Bourreille, A., Le Dily, S., Vavasseur, F., ... & Derkinderen, P. (2015). Structural alterations of the intestinal epithelial barrier in Parkinson's disease. *Acta neuropathologica communications*, *3*(1), 1-9. -3
18. Tsukita, S. (2013). *Tight Junctions. Encyclopedia of Biological Chemistry, 392–395.* doi:10.1016/b978-0-12-378630-2.00440-0
19. Yu, A. S. L., Hanner, F., & Peti-Peterdi, J. (2013). *Intercellular Junctions. Seldin and Giebisch's The Kidney, 347–368.* doi:10.1016/b978-0-12-381462-3.00012-4
20. Lian, P., Braber, S., Garssen, J., Wichers, H. J., Folkerts, G., Fink-Gremmels, J., & Varasteh, S. (2020). Beyond heat stress: intestinal integrity disruption and mechanism-based intervention strategies. *Nutrients*, *12*(3), 734.Fulda, S.; Gorman, A.M.; Hori, O.; Samali, A. Cellular stress responses: Cell survival and cell death. Int. J. Cell Biol. 2010, 2010, 214074. [CrossRef] [PubMed]
21. Fulda, S., Gorman, A. M., Hori, O., & Samali, A. (2010). Cellular stress responses: cell survival and cell death. *International journal of cell biology*, *2010*.
22. Juan, C. A., Pérez de la Lastra, J. M., Plou, F. J., & Pérez-Lebeña, E. (2021). The Chemistry of Reactive Oxygen Species (ROS) Revisited: Outlining Their Role in Biological Macromolecules (DNA, Lipids and Proteins) and Induced Pathologies. *International journal of molecular sciences*, *22*(9), 4642. https://doi.org/10.3390/ijms22094642
23. Lambert, G. P., Gisolfi, C. V., Berg, D. J., Moseley, P. L., Oberley, L. W., & Kregel, K. C. (2002). Selected contribution: Hyperthermia-induced intestinal permeability and the role of oxidative and nitrosative stress. *Journal of applied physiology*, *92*(4), 1750-1761.
24. Costa, R. J. S., Snipe, R. M. J., Kitic, C. M., & Gibson, P. R. (2017). Systematic review: exercise-induced gastrointestinal syndrome—implications for health and intestinal disease. *Alimentary pharmacology & therapeutics*, *46*(3), 246-265.
25. Costa, R., Gaskell, S. K., McCubbin, A. J., & Snipe, R. (2019). Exertional-heat stress-associated gastrointestinal perturbations during Olympic sports: Management strategies for athletes preparing and competing in the 2020 Tokyo Olympic Games. *Temperature (Austin, Tex.)*, *7*(1), 58–88. https://doi.org/10.1080/23328940.2019.1597676
26. Lian, P., Braber, S., Varasteh, S., Wichers, H. J., & Folkerts, G. (2021). Hypoxia and heat stress affect epithelial integrity in a Caco-2/HT-29 co-culture. *Scientific reports*, *11*(1), 1-14.
27. Akbarian, A., Michiels, J., Degroote, J., Majdeddin, M., Golian, A., & De Smet, S. (2016). Association between heat stress and oxidative stress in poultry; mitochondrial dysfunction and dietary interventions with phytochemicals. *Journal of animal science and biotechnology*, *7*(1), 1-14.
28. Park, C. M., Reid, P. E., Walker, D. C., & MacPherson, B. R. (1987). A simple, practical 'swiss roll'method of preparing tissues for paraffin or methacrylate embedding. *Journal of microscopy*, *145*(1), 115-120.
29. Erben, U., Loddenkemper, C., Doerfel, K., Spieckermann, S., Haller, D., Heimesaat, M. M., ... & Kühl, A. A. (2014). A guide to histomorphological evaluation of intestinal inflammation in mouse models. *International journal of clinical and experimental pathology*, *7*(8), 4557.
30. Svensson, M., Rosvall, P., Boza-Serrano, A., Andersson, E., Lexell, J., & Deierborg, T. (2016). Forced treadmill exercise can induce stress and increase neuronal damage in a mouse model of global cerebral ischemia. *Neurobiology of stress*, *5*, 8-18.
31. Cook, M. D., Martin, S. A., Williams, C., Whitlock, K., Wallig, M. A., Pence, B. D., & Woods, J. A. (2013). Forced treadmill exercise training exacerbates inflammation and causes mortality while voluntary wheel training is protective in a mouse model of colitis. Brain, Behavior, and Immunity, 33, 46–56. doi:10.1016/j.bbi.2013.05.005

32. Liu, Y. Z., Wang, Y. X., & Jiang, C. L. (2017). Inflammation: the common pathway of stress-related diseases. *Frontiers in human neuroscience*, 316.
33. Sun, Y., Li, L., Xie, R., Wang, B., Jiang, K., & Cao, H. (2019). *Stress Triggers Flare of Inflammatory Bowel Disease in Children and Adults. Frontiers in Pediatrics, 7.* doi:10.3389/fped.2019.00432
34. Habiyambere, Bupe Martha, "Effect of Stress on Mucin Expression in the Gastrointestinal Tract of Mice." (2010). Electronic Theses and Dissertations. Paper 2253. https://dc.etsu.edu/etd/2253
35. Naylor, B. (2008). *Pleural, Peritoneal, and Pericardial Effusions. Comprehensive Cytopathology, 515–577.* doi:10.1016/b978-141604208-2.10019-3
36. Hodges, R. R., & Dartt, D. A. (2010). *Conjunctival Goblet Cells. Encyclopedia of the Eye, 369–376.* doi:10.1016/b978-0-12-374203-2.00053-1
37. Gomes, Jose & Freitas, J.R. & Grassiolli, Sabrina. (2016). Effects of Physical Exercise on the Intestinal Mucosa of Rats Submitted to a Hypothalamic Obesity Condition. The Anatomical Record. 299. 10.1002/ar.23453.
38. Patel, K. K., Miyoshi, H., Beatty, W. L., Head, R. D., Malvin, N. P., Cadwell, K., ... & Stappenbeck, T. S. (2013). Autophagy proteins control goblet cell function by potentiating reactive oxygen species production. *The EMBO journal*, *32*(24), 3130-3144.
39. Kim, Y. S., & Ho, S. B. (2010). Intestinal goblet cells and mucins in health and disease: recent insights and progress. *Current gastroenterology reports*, *12*(5), 319-330.
40. Tang, D., Wu, J., Jiao, H., Wang, X., Zhao, J., & Lin, H. (2018). *The development of antioxidant system in the intestinal tract of broiler chickens. Poultry Science.* doi:10.3382/ps/pey415 – GSH decrease trought the small intestine
41. Brownlee, I. A., Knight, J., Dettmar, P. W., & Pearson, J. P. (2007). *Action of reactive oxygen species on colonic mucus secretions. Free Radical Biology and Medicine, 43(5), 800–808.* doi:10.1016/j.freeradbiomed.2007.
42. Petersen Shay, K., Moreau, R. F., Smith, E. J., & Hagen, T. M. (2008). *Is α-lipoic acid a scavenger of reactive oxygen speciesin vivo? Evidence for its initiation of stress signaling pathways that promote endogenous antioxidant capacity. IUBMB Life, 60(6), 362–367.* doi:10.1002/iub.40
43. Fischer, A. H., Jacobson, K. A., Rose, J., & Zeller, R. (2008). *Hematoxylin and Eosin Staining of Tissue and Cell Sections. Cold Spring Harbor Protocols, 2008(6), pdb.prot4986–pdb.prot4986.* doi:10.1101/pdb.prot4986
44. De Oliveira, E. P., & Burini, R. C. (2009). *The impact of physical exercise on the gastrointestinal tract. Current Opinion in Clinical Nutrition and Metabolic Care, 12(5), 533–538.* doi:10.1097/mco.0b013e32832e6776
45. Mrakic-Sposta, S., Gussoni, M., Porcelli, S., Pugliese, L., Pavei, G., Bellistri, G., ... & Vezzoli, A. (2015). Training effects on ROS production determined by electron paramagnetic resonance in master swimmers. *Oxidative Medicine and Cellular Longevity*, *2015*.
46. Sproston, N. R., & Ashworth, J. J. (2018). Role of C-reactive protein at sites of inflammation and infection. *Frontiers in immunology*, *9*, 754.
47. Wang, Y., Chen, Y., Zhang, X., Lu, Y., & Chen, H. (2020). *New insights in intestinal oxidative stress damage and the health intervention effects of nutrients: A review. Journal of Functional Foods, 75, 104248.* doi:10.1016/j.jff.2020.104248
48. Im, K., Mareninov, S., Diaz, M., & Yong, W. H. (2019). An introduction to performing immunofluorescence staining. *Biobanking*, 299-311.
49. Manda, B. (2016). *Role of Occludin in the Regulation of Epithelial Tight Junctions* (Doctoral dissertation, The University of Tennessee Health Science Center).
50. Al-Sadi, R., Khatib, K., Guo, S., Ye, D., Youssef, M., & Ma, T. (2011). Occludin regulates macromolecule flux across the intestinal epithelial tight junction barrier. *American Journal of Physiology-Gastrointestinal and Liver Physiology*, *300*(6), G1054-G1064.
51. Saito, A. C., Higashi, T., Fukazawa, Y., Otani, T., Tauchi, M., Higashi, A. Y., ... & Chiba, H. (2021). Occludin and tricellulin facilitate formation of anastomosing tight-junction strand network to improve barrier function. *Molecular biology of the cell*, *32*(8), 722-738.

52. Chelakkot, C., Choi, Y., Kim, D. K., Park, H. T., Ghim, J., Kwon, Y., ... & Ryu, S. H. (2018). Akkermansia muciniphila-derived extracellular vesicles influence gut permeability through the regulation of tight junctions. *Experimental & molecular medicine*, *50*(2), e450-e450.
53. Coëffier, M., Gloro, R., Boukhettala, N., Aziz, M., Lecleire, S., Vandaele, N., ... & Ducrotté, P. (2010). Increased proteasome-mediated degradation of occludin in irritable bowel syndrome. *Official journal of the American College of Gastroenterology| ACG*, *105*(5), 1181-1188.
54. Shen, L. (2012). Tight junctions on the move: molecular mechanisms for epithelial barrier regulation. Annals of the New York Academy of Sciences, 1258(1), 9–18. doi:10.1111/j.1749-6632.2012.06613.x
55. Milatz, S., Krug, S. M., Rosenthal, R., Günzel, D., Müller, D., Schulzke, J. D., ... & Fromm, M. (2010). Claudin-3 acts as a sealing component of the tight junction for ions of either charge and uncharged solutes. *Biochimica et Biophysica Acta (BBA)-Biomembranes*, *1798*(11), 2048-2057.
56. Wang, F., Graham, W. V., Wang, Y., Witkowski, E. D., Schwarz, B. T., & Turner, J. R. (2005). Interferon-γ and tumor necrosis factor-α synergize to induce intestinal epithelial barrier dysfunction by up-regulating myosin light chain kinase expression. *The American journal of pathology*, *166*(2), 409-419.
57. Haines, R. J., Beard, R. S., Chen, L., Eitnier, R., & Wu, M. H. (2016). IL-1β activation of non-muscle myosin light chain kinase mediates β-catenin driven downregulation of claudin-3 and barrier dysfunction in Caco2 cells. *Digestive diseases and sciences*, *61*(8), 2252.
58. Tokuhara, Y., Morinishi, T., Matsunaga, T., Sakai, M., Sakai, T., Ohsaki, H. ... Hirakawa, E. (2018). Nuclear expression of claudin-3 in human colorectal adenocarcinoma cell lines and tissues. Oncology Letters, 15, 99-108. https://doi.org/10.3892/ol.2017.7281
59. Lin, S., Li, Y., Zamyatnin, A. A., Werner, J., & Bazhin, A. V. (2018). Reactive oxygen species and colorectal cancer. Journal of Cellular Physiology, 233(7), 5119–5132. doi:10.1002/jcp.26356
60. Lee, B., Moon, K. M., & Kim, C. Y. (2018). Tight junction in the intestinal epithelium: its association with diseases and regulation by phytochemicals. *Journal of immunology research*, *2018*.
61. Poritz, L. S., Garver, K. I., Green, C., Fitzpatrick, L., Ruggiero, F., & Koltun, W. A. (2007). *Loss of the Tight Junction Protein ZO-1 in Dextran Sulfate Sodium Induced Colitis. Journal of Surgical Research, 140(1), 12–19.* doi:10.1016/j.jss.2006.07.050
62. Markov, A. G., Veshnyakova, A., Fromm, M., Amasheh, M., & Amasheh, S. (2010). Segmental expression of claudin proteins correlates with tight junction barrier properties in rat intestine. *Journal of Comparative Physiology B*, *180*(4), 591-598.
63. Volynets, V., Rings, A., Bárdos, G., Ostaff, M. J., Wehkamp, J., & Bischoff, S. C. (2016). *Intestinal barrier analysis by assessment of mucins, tight junctions, and α-defensins in healthy C57BL/6J and BALB/cJ mice. Tissue Barriers, 4(3), e1208468.* doi:10.1080/21688370.2016.1208468

Supplementary information

Info S1. The ingredients of each diet from the second batch

SM M-Z, 10 mm, Placebo

Crude Nutrients: Crude protein-22.0%; Crude fat-4.5%; Crude fiber-3.9%; Crude ash-6.7%; Starch-34.9%; Sugar-5.2%.

Nutritional feed additives per kg: Vitamin A (3a672a] 25,000 IU; Vitamin Da[3a671] 1,500 IU; Vitamin E (3a700) 125 mg; Vitamin Ka 20 mg: Vitamin C (3a300)- mg; Iron, Ferrous sulphate monohydrate [3b103] 100 mg; Zinc, Zinc sulphate monohydrate [3b605] 50 mg; Manganese, Manganous (Il)-sulphate monohydrate [3b503] 30 mg; Copper, Copper(If)-sulfate pentahydrate [3b405] 5 mg: Selenium, Sodium selenite [3b801] 0.1 mg; lodine, Calcium iodate anhydrous [3b202] 2.0 mg.

SM M, V1124 | +0.4 % Resveratrol 10 mm

Crude Nutrients: Crude protein-22.0%; Crude fat-4.5%; Crude fiber-3.9%; Crude ash-6.7%; Starch-34.9%; Sugar-5.2%.

Nutritional feed additives per kg: Vitamin A (3a672a) 25,000 IU; Vitamin Da (3a671] 1,500 IU; Vitamin E (3a700) 250 mg; Vitamin K: 20 mg; Vitamin C13a3001- mg; Iron, Ferrous sulphate monohydrate [3b103] 100 mg; Zinc, Zine sulphate monohydrate (3b605) 50 mg; Manganese, Manganous (Il)-sulphate monohydrate (3b503) 30 mg; Copper, Copper(I)-sultate pentahydrate (3b405) 5 mg; Selenium, Sodium selenite (3b801] 0.1 mg; lodine, Calcium iodate anhydrous (3b202) 2.0 mg.

SM M, V1124 | +0.20 % a-Lipoic acid [CAS 1077-28-71] - 10 mm

Crude Nutrients: Crude protein-22.0%; Crude fat-4.5%; Crude fiber-3.9%; Crude ash-6.7%; Starch-34.9%; Sugar-5.2%.

Nutritional feed additives per kg: Vitamin A [3a672a] 25,000 IU; Vitamin Da (32671) 1,500 IU; Vitamin E [3a700] 250 mg; Vitamin Ka 20 mg; Vitamin C [3a300].- mg; Iron, Ferrous sulphate monohydrate (3b103) 100 mg; Zinc, Zinc sulphate monohydrate [3b605] 50 mg; Manganese, Manganous(11)-sulphate monohydrate [3b503] 30 mg; Copper, Copper(I)-sulfate pentahydrate [3b405] 5 mg; Selenium, Sodium selenite [3b801] 0.1 mg; lodine, Calcium iodate anhydrous (3b202] 2.0 mg.

Table S1. The ingredients of RM3 (P) standard chow diet.

Nutrients	**Unit**	**Total**	**Supp. [9]**
Proximate Analysis			
Moisture [1]	%	10.00	
Crude Oil	%	4.20	
Crude Protein	%	22.45	
Crude Fibre	%	4.42	
Ash	%	8.05	
Nitrogen Free Extract	%	50.40	
Digestibility Co-Efficients [7]			
Digestible Crude Oil	%	3.81	
Digestible Crude Protein	%	20.18	
Carbohydrates, Fibre and Non Starch Polysaccharides			
Total Dietary Fibre	%	16.15	
Pectin	%	1.53	
Hemicellulose	%	9.61	

Cellulose	%	4.13	
Lignin	%	1.54	
Starch	%	33.88	
Sugar	%	4.37	
Energy [5]			
Gross Energy	MJ/kg	15.11	
Digestible Energy [10]	MJ/kg	12.22	
Metabolisable Energy [10]	MJ/kg	11.18	
Atwater Fuel Energy (AFE) [8]	MJ/kg	13.76	
AFE from Oil	%	11.48	
AFE from Protein	%	27.28	
AFE from Carbohydrate	%	61.24	
Fatty Acids *Saturated Fatty Acids*			
C12:0 Lauric	%	0.05	
C14:0 Myristic	%	0.17	
C16:0 Palmitic	%	0.37	
C18:0 Stearic	%	0.11	
Monounsaturated Fatty Acids			
C14:1 Myristoleic	%	0.01	
C16:1 Palmitoleic	%	0.09	
C18:1 Oleic	%	1.01	
Polyunsaturated Fatty Acids			
C18:2 (ω6) Linoleic	%	1.26	
C18:3 (ω3) Linolenic	%	0.17	
C20:4 (ω6) Arachidonic	%	0.12	
C22:5 (ω3) Clupanodonic	%		

Amino Acids			
Arginine	%	1.42	
Lysine [6]	%	1.34	0.18
Methionine	%	0.37	0.03
Cystine	%	0.35	
Tryptophan	%	0.27	
Histidine	%	0.55	
Threonine	%	0.88	
Isoleucine	%	0.98	
Leucine	%	1.87	
Phenylalanine	%	1.23	
Valine	%	1.15	
Tyrosine	%	0.87	
Taurine	%		
Glycine	%	1.85	
Aspartic Acid	%	1.40	
Glutamic Acid	%	4.39	
Proline	%	1.56	
Serine	%	1.01	
Hydroxyproline	%		
Hydroxylysine	%		
Alanine	%	0.27	
Macro Minerals			
Calcium	%	1.24	1.11
Total Phosphorus	%	0.83	0.28
Phytate Phosphorus	%	0.26	
Available Phosphorus	%	0.56	0.28

Sodium	%	0.24	0.19
Chloride	%	0.36	0.31
Potassium	%	0.81	
Magnesium	%	0.29	0.04
Micro Minerals			
Iron	mg/kg	163.44	82.50
Copper	mg/kg	20.53	8.75
Manganese	mg/kg	102.71	52.70
Zinc	mg/kg	48.67	8.64
Cobalt	µg/kg	604.44	525.00
Iodine	µg/kg	867.77	775.00
Selenium	µg/kg	388.94	200.00
Fluorine	mg/kg	8.67	
Vitamins			
β-Carotene [2]	mg/kg	1.67	
Retinol [2]	µg/kg	6670.95	5812.5
Vitamin A [2]	iu/kg	22213.06	19375
Cholecalciferol [3]	µg/kg	73.70	72.50
Vitamin D [3]	iu/kg	2948.01	2900
α-Tocopherol [4]	mg/kg	100.9	81.14
Vitamin E [4]	iu/kg	111.02	89.25
Vitamin B_1 (Thiamine)	mg/kg	28.39	19.11
Vitamin B_2 (Riboflavin)	mg/kg	10.28	7.60
Vitamin B_6 (Pyridoxine)	mg/kg	18.87	14.45
Vitamin B_{12} (Cyanocobalamine)	µg/kg	19.23	17.75
Vitamin C (Ascorbic Acid)	mg/kg	1.33	
Vitamin K (Menadione)	mg/kg	4.14	3.72

Folic Acid (Vitamin B_9)	mg/kg	2.99	0.49
Nicotinic Acid (Vitamin PP) [6]	mg/kg	85.74	19.11
Pantothenic Acid (Vitamin $B_{3/5}$)	mg/kg	40.79	23.80
Choline (Vitamin $B_{4/7}$)	mg/kg	1422.37	366.60
Inositol	mg/kg	1839.97	
Biotin (Vitamin H) [6]	µg/kg	316.66	

1. All values are calculated using a moisture basis of 10%. Typical moisture levels will range between 9.5 - 11.5%.

2. (a) Vitamin A includes Retinol and the Retinol equivalents of β-carotene. (b) Retinol includes the Retinol equivalents of β-Carotene. (c) 0.48 µg Retinol = 1 µg β-carotene = 1.6 iu Vitamin A activity. (d) 1 µg Retinol = 3.33 × iu Vitamin A activity. (e) 1 iu Vitamin A = 0.3 µg Retinol = 0.6 µg β-carotene. (f) The standard analysis for Vitamin A does not detect β-carotene.

3. 1 µg Cholecalciferol (D_3)=40.0 iu Vitamin D

4. 1 mg all-*rac*-α-tocopherol = 1.1 iu Vitamin E activity. 1 mg all-*rac*-α-tocopherol acetate = 1.0 iu Vitamin E activity.

5. 1 MJ = 239.23 Kcalories = 239.23 Calories = 239,230 calories.

6. These nutrients coming from natural raw materials such as cereals may have low availabilities due to the interactions with other compounds.

7. Based on in-vitro digestibility analysis.

8. AF Energy = Atwater Fuel Energy = [(CO% / 100) × 9000] + [(CP% / 100) × 4000] + [(NFE% / 100) × 4000] / 239.23

9. Supplemented nutrients from manufactured and mined sources.

10. Calculated.

Table S2. Exercise training program for the adaptation period.

Day 1

Speed (m/min)	**Time (min)**
0	2
6	3
8	5
10	10

Total time	20
Total distance	158 m
Average speed	7.9 m/min

Day 2

Speed (m/min)	**Time (min)**
0	2
6	3
8	5
10	5
12	15
Total time	30
Total distance	228 m
Average speed	7.6 m/min

Day 3

Moderate		**Intense**	
Speed (m/min)	**Time (min)**	**Speed (m/min)**	**Time (min)**
6	3	6	3
8	4	9	3
10	4	12	2
12	4	15	2
14	30	17	2
		20	2
		23	16
Total time	45	**Total time**	30
Total distance	558 m	**Total distance**	541 m
Average speed	12.4 m/min	**Average speed**	18.0 m/min

Table S3. Exercise training program for the regular training period.

Day 4-14

Moderate		**Intense**	
Speed (m/min)	**Time (min)**	**Speed (m/min)**	**Time (min)**
6	1	10	1
8	2	12	1
10	3	14	1
12	4	17	1
14	5	20	1
16	45	23	25
Total time	60	**Total time**	30
Total distance	890 m	**Total distance**	648 m
Average speed	14.8 m/min	**Average speed**	21.6 m/min

Day 15-28

Moderate		**Intense**	
Speed (m/min)	**Time (min)**	**Speed (m/min)**	**Time (min)**
7	1	11	1
9	2	13	1
11	3	15	1
13	4	18	1
15	5	21	1
17	45	24	25
Total time	60	**Total time**	30
Total distance	950 m	**Total distance**	678 m
Average speed	15.8 m/min	**Average speed**	22.6 m/min

Day 29-42

Moderate		**Intense**	
Speed (m/min)	**Time (min)**	**Speed (m/min)**	**Time (min)**
7	1	12	1
9	2	14	1
11	3	16	1
13	4	19	1
15	5	22	1
17	45	25	25
Total time	60	**Total time**	30
Total distance	950 m	**Total distance**	708 m
Average speed	15.8 m/min	**Average speed**	23.6 m/min

Table S4. Scoring scheme for colonic morphology.

Inflammatory cell infiltrate		**Score**
Severity	**Extent**	
Minimal	Mucosa	1
Mild	Mucosa and submucosa	2
Moderate	Mucosa and submucosa, sometimes transmural	3
Marked	Mucosa and submucosa, often transmural	4
Epithelial changes		
Minimal hyperplasia		1
Mild hyperplasia, minimal goblet cell loss		2
Moderate hyperplasia, mild goblet cell loss		3
Marked hyperplasia with moderate to marked goblet cell loss		4
Mucosal architecture		

Ulceration, irregular crypts or crypt loss (only one is seen)	3
Ulceration, irregular crypts and crypt loss (at least two are combined)	4

Sum of scores: 0-12

Table S5. Scoring scheme for proximal and distal small intestine morphology.

Inflammatory cell infiltrate		**Score**
Severity	**Extent**	
Mild	Mucosa and sometimes submucosa	1
Moderate	Mucosa and submucosa	2
Marked	Mucosa and submucosa, sometimes transmural	3
Marked	Mucosa and submucosa, often transmural	4
Epithelial changes		
Mild hyperplasia, minimal goblet cell loss		2
Moderate hyperplasia, mild goblet cell loss		3
Marked hyperplasia and goblet cell loss		4

Mucosal architecture	
Mild villous blunting	1
Moderate villous blunting	2
Moderate villous blunting and broadening, sometimes villous atrophy; crypt loss	3
Ulceration, villous atrophy and crypt loss	4

Sum of scores: 0-12

Table S5. Serum CRP concentration in response to 6 weeks of sedentary (CON), moderate exercise (MOD-EX) or vigorous exercise (VIG-EX) .

Analyte	**Serum cytokine/chemokine concentration**		
	CON (pg/ml)	**MOD-EX (pg/ml)**	**VIG-EX (pg/ml)**
CRP	11328 ± 617	17210 ± 1140 **	14092 ± 1635

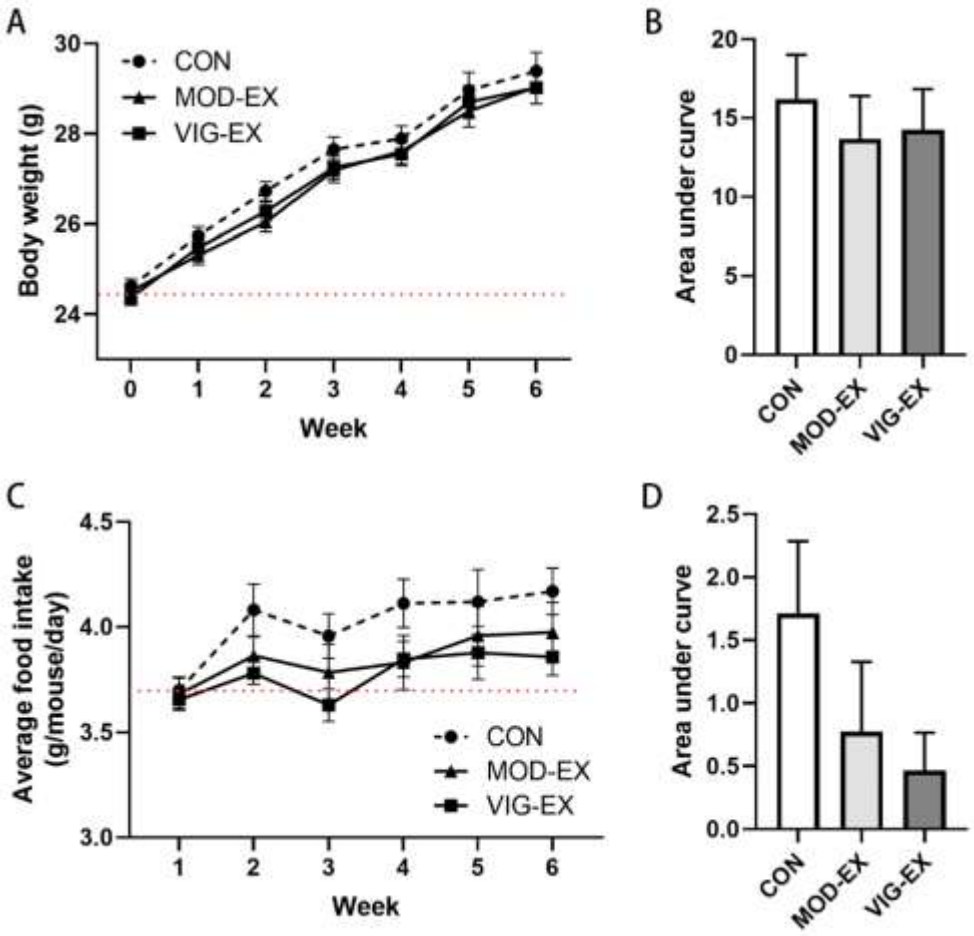

Figure S1. Effect of two intensities of treadmill running on body weight and food intake. (**A** and **B**) Body weight gain and integral area under the curves of body weight calculated for statistical analysis. The red dotted-line represents the baseline: the average body weight of all mice at week 0 (24.63 g). Data are presented as mean ± SEM; n = 20 (individuals) per group. (**C** and **D**) Average food intake per day and integral area under the curves of food intake calculated for statistical analysis. The red dotted-line represents the baseline: the average daily food intake per mouse of Control at week 1 (3.70 g). Data are presented as mean ± SEM; n = 5 (cages) per group. Statistical differences were analyzed by one-way ANOVA followed by the Bonferroni's multiple comparison test. No significant differences of means were observed between the groups of interest ($p > 0.05$). CON: Control; MOD-EX: Moderate Exercise; VIG-EX: Vigorous Exercise.

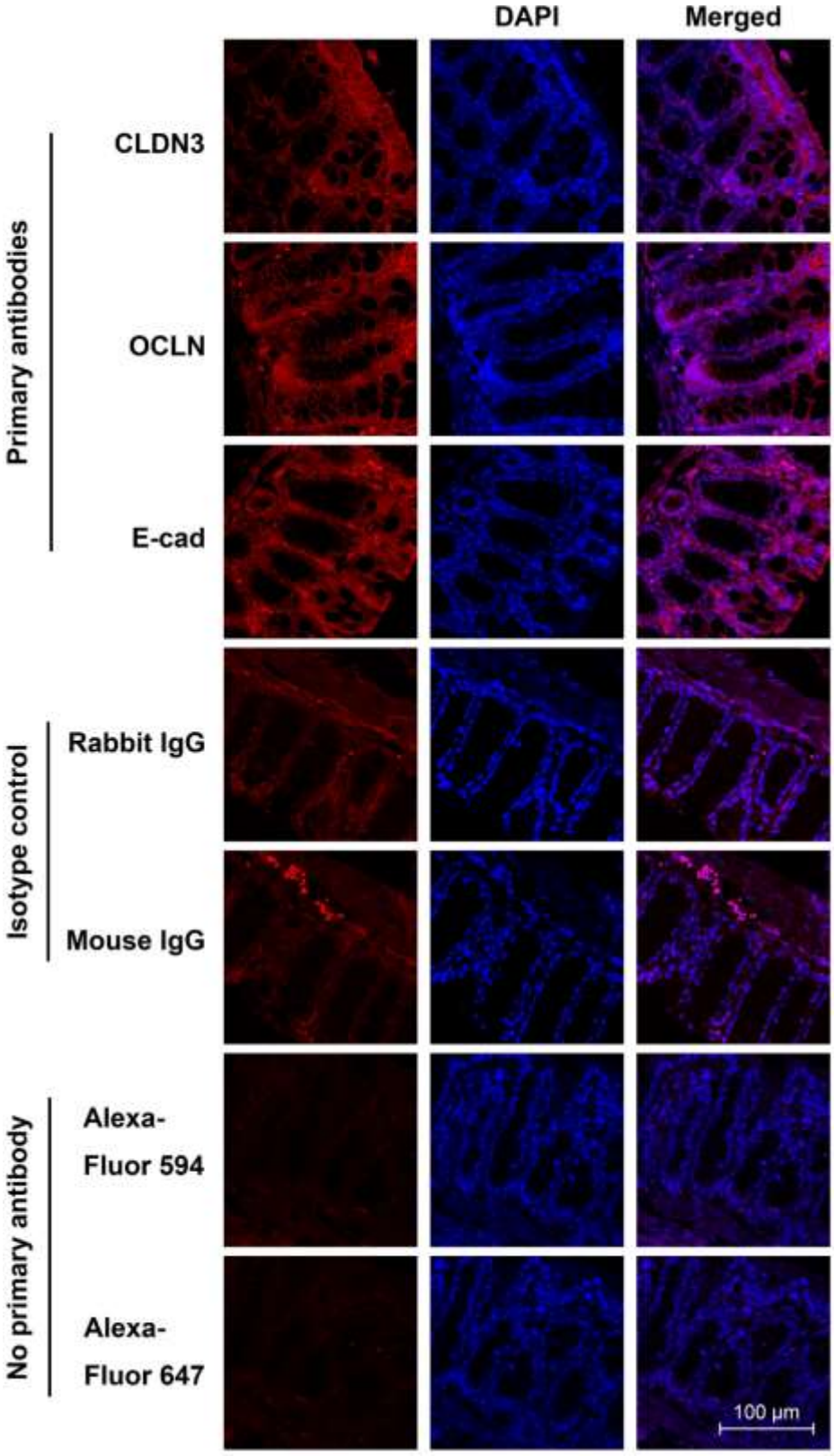

Figure S2. Isotype control and secondary antibody control of the immunofluorescence staining. The results were acquired by Leica TCS SP8 confocal microscope with HCX IRAPO L 25×/0.95 objective lens at 2.25× digital

magnification; pinhole: 1.50 AU. Red colour: fluorescent signals from Alexa-Fluor® 594 or Alexa-Fluor® 647 secondary antibodies; blue colour: DAPI located nuclei. CLDN3: claudin-3; OCLN: occludin; E-cad: E-cadherin.

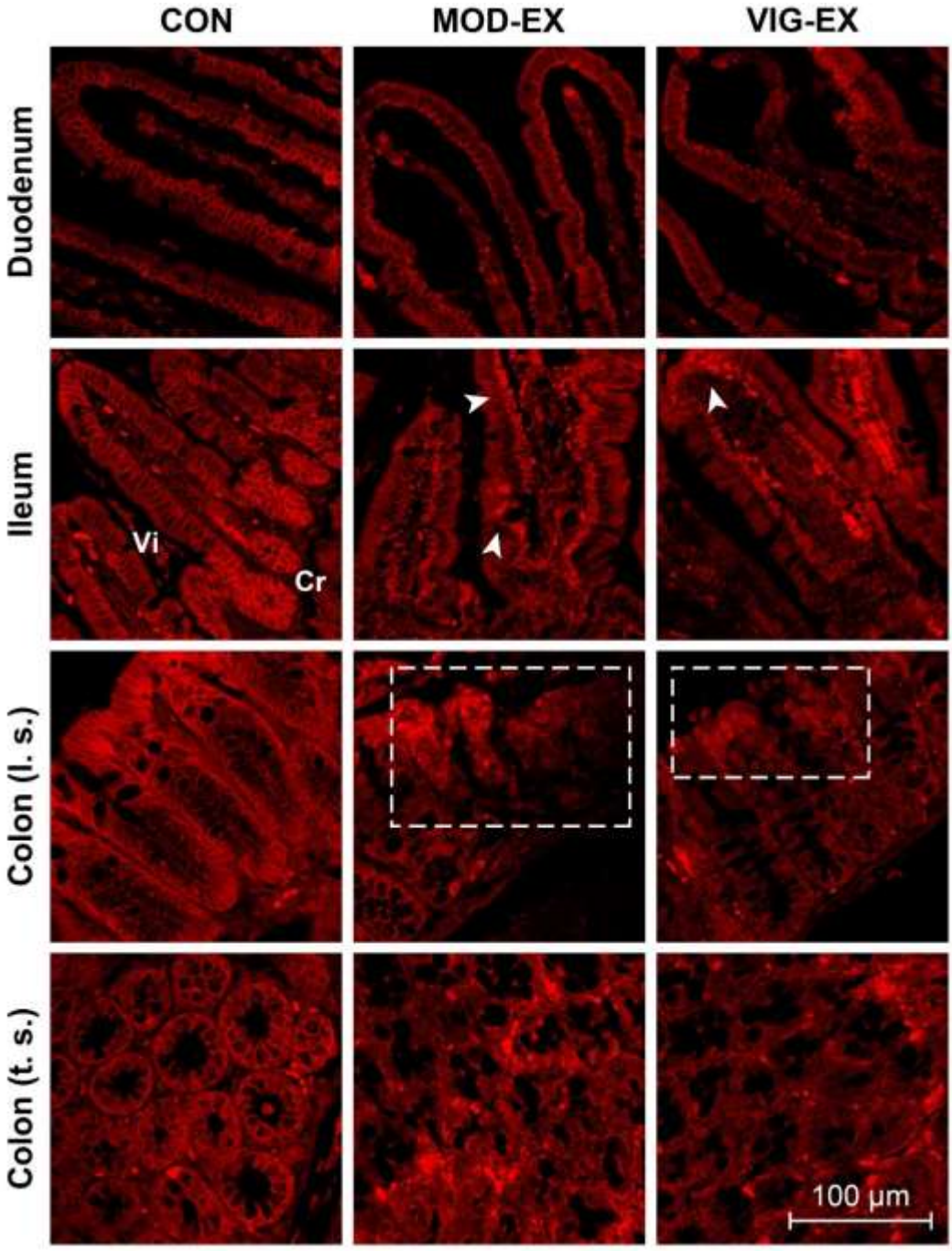

Figure S3. Immunofluorescence staining of duodenal, ileal and colonic occludin protein. In the sedentary mice, OCLN localized at the cell membrane and showed continuous chain-like structures forming the rim of duodenal and ileal villi. There were stronger OCLD expression observed in ileal crypts (Cr) than in villi (Vi). Strenuous exercise-exposed duodenum and ileum exhibited disturbed continuity of the villous margin. The chain-like structures and strong crypt OCLN expression are less clear to observe. In addition, OCLN tended to aggregate on the lamina propria side (arrow heads), which might indicate the translocation of OCLN protein. The results were acquired by Leica TCS SP8 confocal microscope with HCX IRAPO L 25×/0.95 objective lens at 2.25× digital magnification;

pinhole: 1.50 AU. Red colour: fluorescent signals from Alexa-Fluor® 594 secondary antibodies; arrow head: aggregative dislocation of occludin; rectangular dashed frame: area indicating the loss of brush-like structure. CON: Control; MOD-EX: Moderate Exercise; VIG-EX: Vigorous Exercise; l.s.: longitudinal section; t.s.: transverse section.

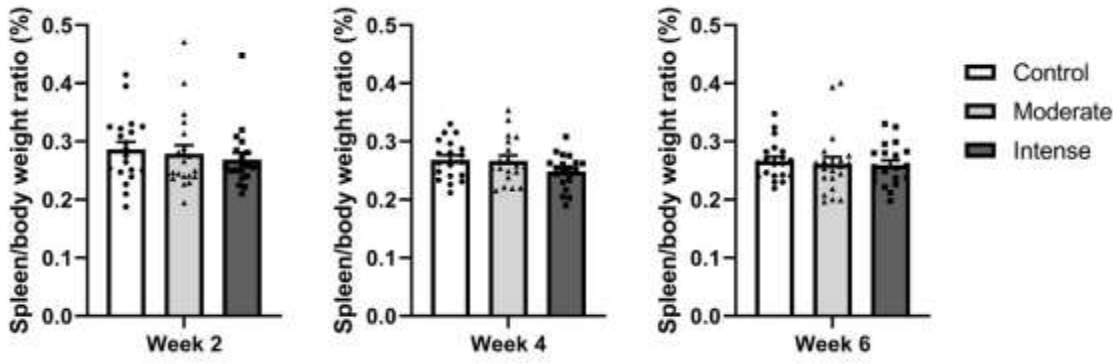

Figure S4. Spleen/body weight ratio of the mice at week 2, 4 and 6. Data are presented as mean ± SEM; n = 20 per group. No significant difference was observed between the groups ($p > 0.05$).

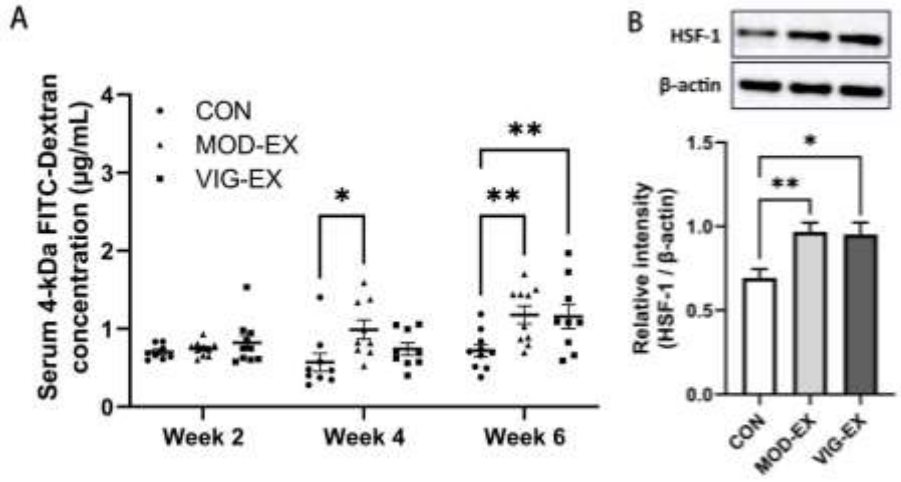

Figure S5 A) Serum 4-kDa FITC-Dextran concentration 1 hour after gavage at week 2, 4 and 6 **B)** Relative protein expression of HSF-1 at week 6 assessed by Western Blot. All target proteins were normalized to reference protein β-actin. Data are presented as mean ± SEM; n = 10 per group. Statistical differences were analyzed by one-way ANOVA followed by the Bonferroni's multiple comparison test. * $p < 0.05$, ** $p < 0.01$,. CON: Control; MOD-EX: Moderate Exercise; VIG-EX: Vigorous Exercise; HSF: heat shock factor.

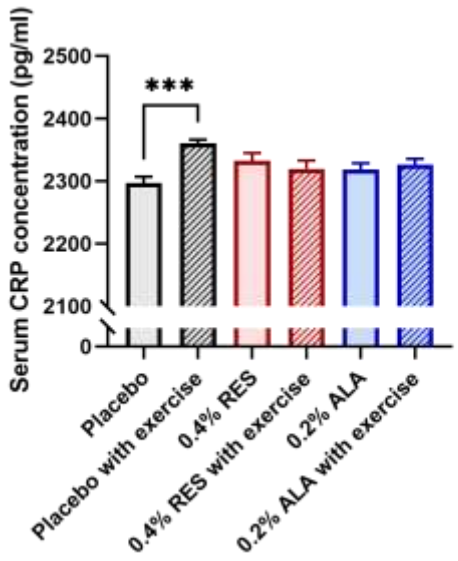

Figure S6. Serum CRP concentration in response to 6 weeks of strenuous exercise and a diet with Placebo, Resveratrol and α-lipoic acid. Data are presented as mean ± SEM; n = 10 per group. Statistical differences were analyzed by one-way ANOVA followed by the Bonferroni's multiple comparison test. *** p<0.001 RES: Resveratrol; ALA: α-lipoic acid

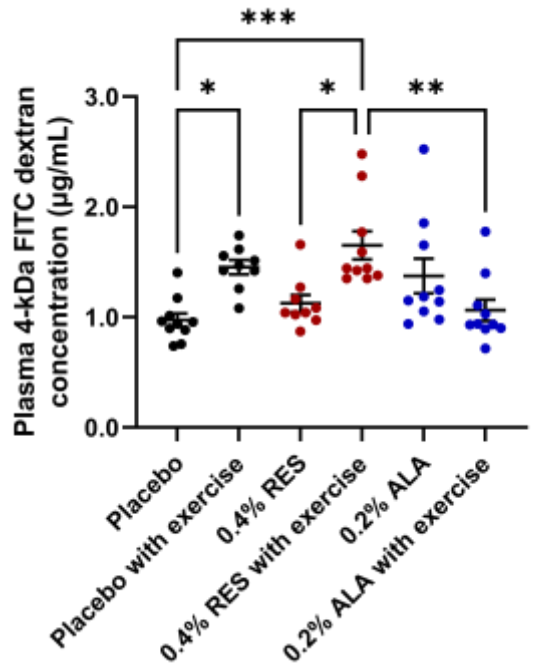

Figure S7. Serum 4-kDa FITC-Dextran concentration 1 hour after gavage at week 2, 4 and 6. Data are presented as mean ± SEM; n = 10 per group. Statistical differences were analyzed by one-way ANOVA followed by the Bonferroni's multiple comparison test. * p < 0.05, ** p < 0.01, *** p < 0.001 RES: Resveratrol; ALA: α-lipoic acid